Negative Phototaxis of Euglena Gracilis and Resulting Bioconvection Patterns under Stationary or Rapidly Periodic Illumination

Dissertation

zur Erlangung des Grades eines
Doktors der Naturwissenschaften

eingereicht am Fachbereich Mathematik und Informatik
der Freien Universität Berlin

vorgelegt von

Yuya Moses Tokuta

Berlin, Mai 2019

Erstgutachter und Betreuer:
Prof. Dr. Bernold Fiedler, Freie Universtät Berlin

Zweitgutachter:
Prof. Dr. Toshiyuki Ogawa, Meiji University

Datum der Disputation:
12. Juli 2019

In so far as a scientific statement speaks about reality, it must be falsifiable: and in so far as it is not falsifiable, it does not speak about reality.

Sir Karl Raimund Popper

Acknowledgment

I would like to express my special thanks of gratitude to Prof. Bernold Fiedler. He welcomed me to his research group immediately after I arrived in Berlin and helped me to make a smooth transition. The research environment has been wonderful and I am convinced that I am very fortunate.

I would also like to thank every member of the research group for both academic and personal interactions. Especially, I am grateful to Nikita Begun, Jia-Yuan Dai, Phillipo Lappicy, Alejandro López Nieto, Isabelle Schneider, Hannes Stuke, Nicola Vassena, and Babette de Wolff, who saved my thesis by giving me a lot of feedback on my early drafts. Adem Güngör helped me with my german abstract.

A word of thanks goes to Prof. Toshiyuki Ogawa and Prof. Nobuhiko J. Suematsu at Meiji University, Japan. An exchange of views and ideas, both online and offline, over the past five years has been fruitful. Prof. Toshiyuki Ogawa also took on the role of the second reviewer of this thesis.

Last but not least, I would like to thank my family and friends. Especially, I would like to thank my wife Miki Tokuta. Thank you for loving me.

This work is partially supported by the Student Exchange Support Program (Graduate Scholarship for Degree Seeking Students) of the Japan Student Services Organization, SFB 910 Project A9: Reaction-diffusion systems: hysteresis and non-local interactions, Berlin Mathematical School Phase II Scholarship, and SFB 910 Project A4: Spatio-temporal patterns: control, delays, and design.

Abstract

By means of modeling and mathematical analysis, this thesis investigates negative phototaxis of Euglena gracilis and resulting bioconvection patterns under stationary or periodic illumination.

This thesis provides a new biological hypothesis about the mechanism of negative phototaxis of Euglena gracilis and gives an account of the failure of pattern formation under rapidly periodic illumination which was reported by an experimentalist.

An existing model of patterns under stationary illumination is extended to a new model of patterns not only under stationary illumination but also under rapidly periodic illumination. The new model has Turing instability for coefficients corresponding to stationary illumination, and loses Turing instability if coefficients are replaced by those corresponding to rapidly periodic illumination. The failure of pattern formation under rapidly periodic illumination can be interpreted as the loss of Turing instability.

Contents

List of Figures

List of Tables

Chapter 1

Introduction

Microbes form spatiotemporal patterns. Among such, cells of Euglena gracilis, a species of single-celled photosensitive flagellate whose diagram is shown in Figure 1.1, form a macroscopic pattern like Figure 1.2 when illuminated [SAI$^+$11].

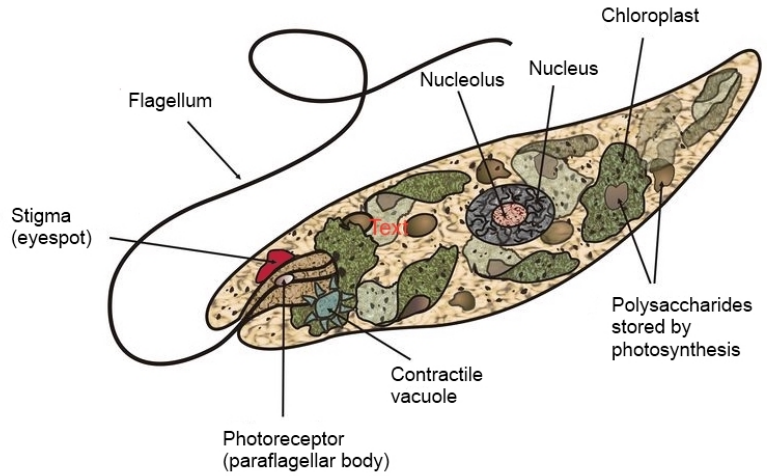

Figure 1.1: Diagram of a cell of Euglena gracilis.

Confined in a sealed container, made by two glass plates and a silicon rubber with a hole placed between the plates, cells swim vertically upward when illuminated by bright light from below. Vertical swimming results in the accumulation of cells near the top glass. Once arriving at the top glass, cells can no longer continue swimming upward, and make a change of direction, followed by horizontal swimming. As a result of horizontal swimming, at points where there are too many cells meeting together, sinking of cells by gravity occurs. A two-component system of reaction-diffusion equations was proposed in [SAI$^+$11] as a model of the collective behavior of cells.

Afterward, Suematsu, an author of the paper [SAI$^+$11], also found that, such a pattern does not emerge under certain periodically fluctuating light. Specifically, no pattern was formed under periodic illumination of frequency around 1Hz; whereas

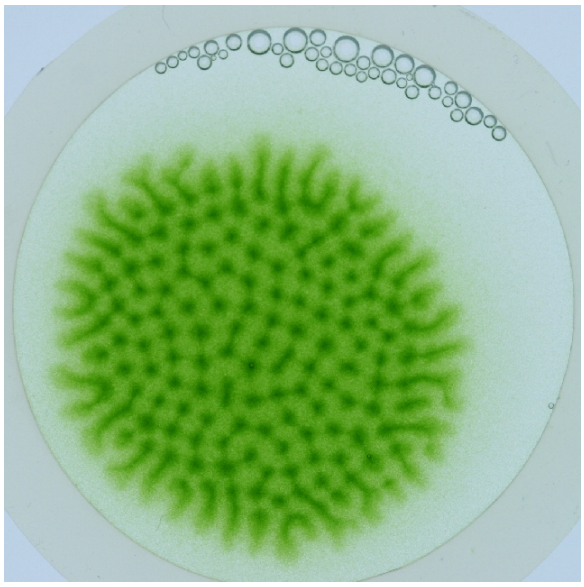

Figure 1.2: Euglena bioconvection ©Nobuhiko J. Suematsu
Real picture taken in the laboratory. View from the top of the sealed container. Darker green signifies higher concentration of cells.

similar patterns were formed under periodic illumination of frequency higher or lower than above range of frequencies.

We want to know why cells fail to form a pattern on this condition. To answer this question, we will build a model designed for both patterns under stationary illumination and periodic illumination. We will analyze the model to find mathematical structure of pattern formation or the failure of pattern formation. To build the model of patterns valid for both illumination conditions, we need a better understanding of negative phototaxis of Euglena gracilis.

To try to understand negative phototaxis better, we will perform a thought experiment based on biological properties of a cell of Euglena gracilis, which can be found in [SS17], and form a hypothesis about the mechanism of negative phototaxis, and build a new model based on the hypothesis.

Mathematical analysis of the model will provide us with a theory of the failure of pattern formation under periodic illumination. The underlying belief is that the real-world phenomena in nature are governed by simple laws written in the language of mathematics.

1.1 Phototaxis of Euglena gracilis

In this section, we introduce responses cells of Euglena gracilis exhibit when exposed to illumination. We refer to [SS17] which covers biochemical, cellular, and molecular biological studies on not only Euglena gracilis but also other species of Euglena in

general. A description of photomovement of Euglena gracilis can be found in Chapter 11.

Motile microorganisms such as Euglena gracilis use a number of external stimuli to orient in their environment. As a result, cells accumulate in suitable habitats and form visible macroscopic patterns.

- Cells of Euglena gracilis move toward the light source at low irradiance as light is necessary for photosynthesis and such response is called **positive phototaxis**. On the other hand, excessive radiation can be detrimental, and cells move away from the light source at high irradiance and such response is called **negative phototaxis**.

- Upon a sudden decrease in light intensity cells show a **step-down photophobic response** which may be a stop, a change in swimming direction or a reversal of movement. Likewise, a sudden increase in the ambient light intensity may result in a **step-up photophobic response** which may be a sudden increase in light intensity which would occur when an organism enters a irradiated area from a shaded one.

- The dependence of the swimming speed on the ambient irradiance is called **photokinesis**.

The paraflagellar body which is at the root of the flagellum (see Figure 1.1) has been identified as the light responsive organelle. Henceforth in this thesis, **we simply call the paraflagellar body the sensor**.

While swimming in the direction of its flagellum, a cell rotates at about 1 Hz around its long axis. See Figure 1.3. The axis itself tumbles erratically within a cone of a 15° opening angle [SS17]. Due to the rotation, the stigma which is next to the sensor (see Figure 1.1) may shade the sensor from illumination; if light comes from the side, the sensor receives flicker, and if light comes from the front or the back, the sensor does not receive flicker.

Stigmaless mutants, however, can also orient with respect to the light direction, and negative phototaxis does not need a stigma. In this thesis, however, we assume that the stigma has an important role. Our theory does not necessarily contradict the ability of a cell without a stigma either. For more discussions, see Chapter 5, Subsection 5.1.2 Stigmaless mutants.

In this thesis, we are concerned with negative phototaxis, i.e. the response of cells swimming away from bright light.

1.2 Stationary illumination

Suematsu et al. [SAI+11] reported a macroscopic pattern of cells of Euglena gracilis under stationary illumination, and found similarities between the pattern and Rayleigh-Bénard convection.

Rayleigh-Bénard convection involves a fluid placed between two flat horizontal heat conducting plates. The lower plate temperature is kept higher than the upper

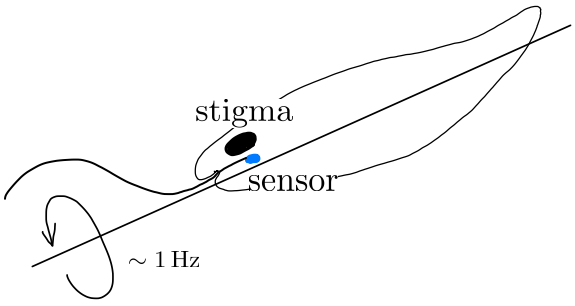

Figure 1.3: The rotation of a cell of Euglena gracilis. Note that the sensor (in blue) is closer to the axis and the stigma (in black) rotates around the sensor.

plate temperature. The fluid near the lower plate becomes less dense due to the thermal expansion, resulting in an intrinsically unstable situation in the gravitational field. Due to conservation of mass, an instability occurs when the heating is so strong that the dissipative effects of thermal conduction and viscosity are dominant. [CH93].

To make a model of the macroscopic convection of Euglena gracilis, Suematsu et al. schematically divided the domain of the sealed container into a thin upper layer and a thick lower layer and studied the exchange of density between the two layers on the cross-section of the container. Based on the experimental observations, Suematsu et al. extracted the following four features of the collective behavior of cells in the cross-section. See Figure 1.4.

(i) Upward vertical movement due to swimming away from bright light from below (negative phototaxis),

(ii) When a cell reaches the top glass, it can no longer continue swimming away. It then makes a change of direction and starts moving horizontally (diffusion in the upper layer); Diffusion in the lower layer was also assumed and it represents the movement in the lateral direction. The lateral movement in the lower layer was considerably weaker than that in the upper layer,

(iii) Sinking due to gravity in the upper layer at points where there are too many cells gathering together, and

(iv) nonlocal decisions of cells in the upper layer, causing lateral swimming, determined by comparing the light intensity to the left and to the right.

As a model of the macroscopic pattern, Suematsu et al. derived a two-component system of reaction-diffusion equations with a nonlocal term:

$$\begin{aligned} \partial_t u &= d_1 \Delta u - \alpha (u+v)^\beta u + cv - \kappa \partial_x [(\psi_+ - \psi_-)u] \\ \partial_t v &= d_2 \Delta v + \alpha (u+v)^\beta u - cv, \end{aligned} \tag{1.1}$$

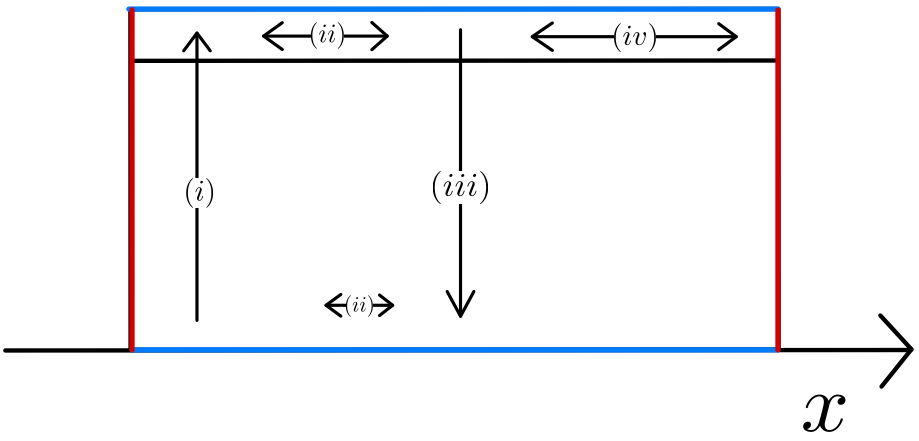

Figure 1.4: Four features of the collective behavior of cells of Euglena gracilis. (i) negative phototaxis, (ii) diffusion in the upper and lower layers, (iii) sinking, and (iv) lateral movement in the upper layer based on nonlocal information. Blue lines represent top and bottom glass and red lines represent silicon rubber walls.

where

$$\begin{aligned} \psi_+ &= \int_x^L u(t,y) \exp\left(-\frac{|x-y|}{\Lambda}\right) dy \\ \psi_- &= \int_0^x u(t,y) \exp\left(-\frac{|x-y|}{\Lambda}\right) dy, \end{aligned} \tag{1.2}$$

with Neumann boundary conditions. Real-valued variables $u(x,t)$ and $v(x,t)$ correspond to the density in the upper layer and lower layer, respectively. The four features shown in Figure 1.4 were represented by the following:

(i) Upward vertical swimming was represented by the loss of the lower layer density v by

$$-cv \tag{1.3}$$

and the gain of the upper layer density u by the same amount. A positive coefficient c determines how much of the lower layer density joins the upper lower density.

(ii) Horizontal swimming once cells arrive at the top glass was represented by diffusion of the upper layer density

$$d_1 \Delta u. \tag{1.4}$$

Horizontal swimming of cells after they sink to the bottom was represented by diffusion of the lower layer density

$$d_2 \Delta v. \tag{1.5}$$

The diffusion rate in the upper layer d_1 was assumed to be much higher than the diffusion rate in the lower layer d_2, i.e. $d_2 \ll d_1$.

(iii) The sinking was assumed to be governed by

$$-\alpha(u+v)^{\beta}u. \tag{1.6}$$

The coefficients α and β were used to approximate some sinking rate function which depends on the sum of the densities on both layers. Here, the primary choice of β is 2 or 3, depending on the resistance while sinking. The prototypes of the resistance are viscous resistance which is of order $\beta \approx 2$; and inertial resistance which is of order $\beta \approx 3$.

(iv) The nonlocal term represented the localization of the pattern, i.e. as in Figure 1.2, patterns were not formed in the whole domain. The coefficient κ is a product of factors coming from several coefficients which were required to derive the nonlocal term. To derive the nonlocal term, Suematsu et al. considered attenuation of light, the self-shading effect, and sensitivity of cells to the gradient of the light intensity.

In this thesis, we will exclude the nonlocal term from our consideration. Suematsu et al. also reports that if the number of cells in the sealed container is high enough, a pattern like Figure 1.2 was formed in the whole domain. See Chapter 5, Subsection 5.3.1 Perturbations for more discussion.

1.3 Periodic illumination

Following the experiment on stationary illumination, the first author Suematsu conducted another experiment on oscillatory illumination. He found that cells of Euglena gracilis failed to form macroscopic patterns under certain periodic illumination. Specifically,

- there existed a range of frequencies of order 1 Hz such that no patterns like Figure 1.2 were formed.
- if the illumination frequency was higher than the above range of frequencies including 1 Hz, patterns like Figure 1.2 were observed.
- if the illumination frequency was lower than the above range of frequencies including 1 Hz, patterns were formed intermittently.

1.4 Main question

The mechanism of the failure of pattern formation has not been given, and we try to give an account of the mechanism, based on a thought experiment on microscopic individual responses, backed up with mathematical treatment of the resulting model.

The main question is the mechanism of Euglena bioconvection. Especially, how cells of Euglena gracilis fail to form a pattern like Figure 1.2 under certain periodic illumination. The key to the problem is an account of negative phototaxis of Euglena gracilis that is valid for both settings, in the individual level. The main question can be reduced to **how cells of Euglena gracilis make use of the information of light their sensors receive**.

We suppose that Euglena bioconvection is a result of an evolution strategy in order to optimize the chances of survival in nature. Their responses must be tuned to the common environment and not to artificial environments such as rapidly periodic illumination from below. If we understand why cells of Euglena gracilis fail to form patterns, we will understand how cells of Euglena gracilis respond to light in general.

1.5 Thought experiment

The range of frequencies of order 1 Hz such that no patterns like Figure 1.2 were formed includes the rotation frequency of individual cells of Euglena gracilis. We study light information the sensor of a cell receives, depending on the environment.

Imagine a cell facing perpendicular to a planar light source as in Figure 1.5.

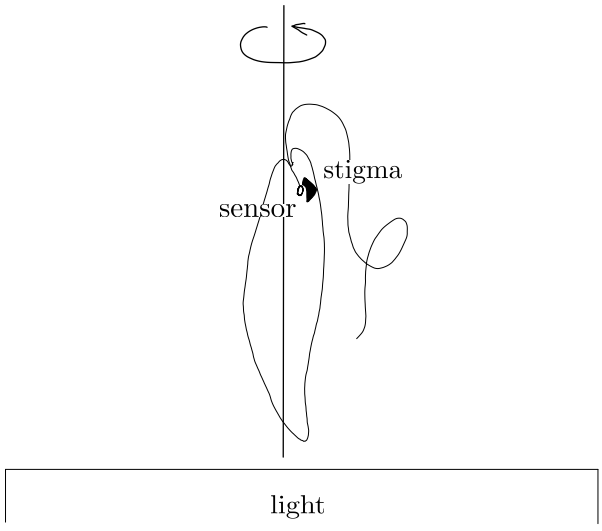

Figure 1.5: A cell facing perpendicular to the planar light source. The sensor will not be shaded by the stigma despite the rotation.

Even though the stigma follows around the sensor, it never blocks the light. Hence, the sensor of a cell receives stationary illumination if the cell is perpendicular.

Next, imagine a cell facing parallel to a planar light source as in Figure 1.6.

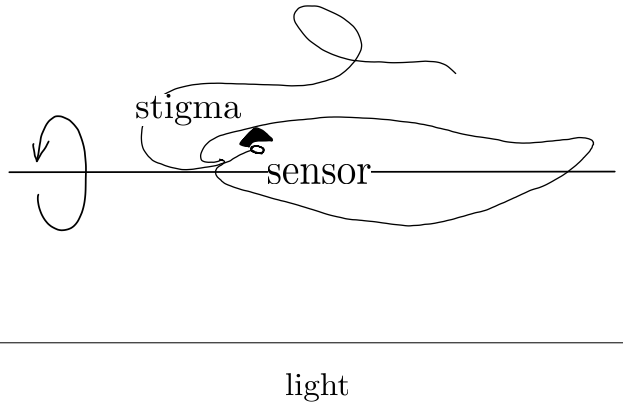

Figure 1.6: A cell facing parallel to the planar light source.The sensor will be shaded by the stigma due to the rotation.

The stigma of a cell blocks the light periodically as the cell rotates. Hence, the sensor of a cell receives periodic illumination if the cell is parallel.

We hypothesize that each cell of Euglena gracilis distinguishes its relative position to the light source by the period of shading of light by its stigma.

- A cell is vertical to the light source if it senses no shading.
- A cells is horizontal to the light source if it senses periodic shading.

To achieve negative phototaxis, a cell must keep facing vertical and continue swimming. In other words, a cell should make a change of direction if it senses periodic shading. On the other hand, a cell should not make a change of direction if it senses no shading.

1.6 Hypothesis

We form the following hypothesis:

> **A cell of Euglena gracilis makes a change of direction if its sensor receives periodic light**. (1.7)

By the change of direction, we mean changing from the vertical position as in Figure 1.7 to the horizontal position as in Figure 1.7; and vice versa. By the periodic light,

we mean periodic light with frequency of order 1 Hz corresponding to the intrinsic frequency of the rotation of a cell.

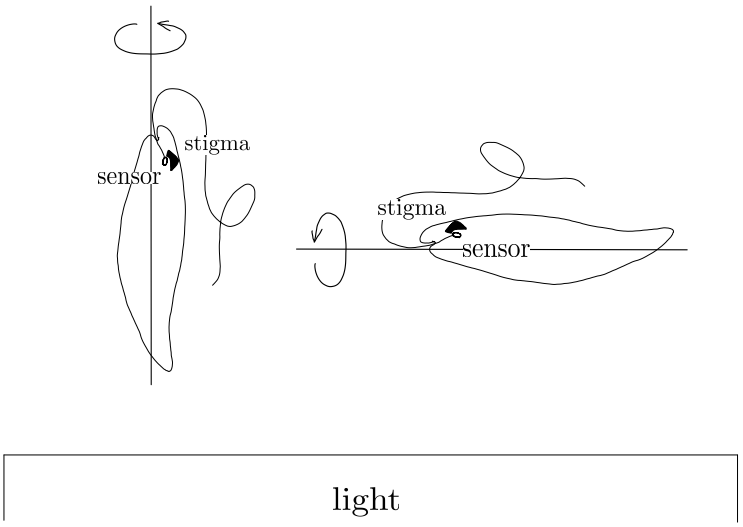

Figure 1.7: Two relative positions of Euglena gracilis we consider in this thesis. We hypothesize that a cell changes the direction upon sensing flicker, resulting in swimming away from light, i.e. negative phototaxis.

Here, we only consider two relative positions, and do not distinguish between a cell facing upward and a cell facing downward. Neither do we distinguish between a cell facing to the right and to the left. We will distinguish between extremely rapidly periodic light and rapidly periodic light.

According to the hypothesis (1.7), in periodic settings, responses of cells to illumination result in a different collective behavior which we will pursue in this thesis.

1.7 Modeling

Based on the hypothesis (1.7), we will derive a model of macroscopic patterns valid for both stationary and periodic settings, generated by their collective behavior depending on the environment.

In principle, we will follow the derivation of the Suematsu model (1.1), but have to deviate from it to accommodate periodic cases.

1.7.1 Time-averaging

In the case of periodic illumination, we have two distinct sources of oscillation:

- external periodic illumination, and

- internal rotation of cells.

The external illumination can be manually controlled, and the frequencies inducing the failure of pattern formation includes the internal rotation frequency of order 1 Hz. We observe that the rotation of cells is rapid in the time-scale of pattern formation. In fact, starting from the initial condition of homogeneous distribution of cells, it took 5-8 min for cells to visibly assemble and form high-density spots at random positions; these spots moved away from the silicon wall and gathered at the center of the container to an ensemble of spots (12-18 min); and repeated fusion and division of the spots as well as migration of spots as an ensemble were observed (20-180 min) [SAI+11].

If we change the illumination conditions from stationary to periodic, a term in the Suematsu model (1.1) corresponding to negative phototaxis has to be modified: Consider a rapidly periodic coefficient

$$c_{\mathrm{per}}(t,\varepsilon) := c[1+\cos(2\pi t/\varepsilon)], \tag{1.8}$$

where $0 < \varepsilon \ll 1$, instead of the stationary coefficient c.

We will study the effect of rapidly periodic forcing on the behavior of solutions to the Suematsu system, using a time-averaging theorem for parabolic partial differential equations under temporal (quasi-)periodic forcing [Mat08], which provides an estimate of the difference between solutions to the system with the rapidly oscillatory coefficient and solutions to the system with the averaged coefficient

$$\langle c_{\mathrm{per}}(t,\varepsilon)\rangle := \frac{1}{\varepsilon}\int_0^{\varepsilon} c_{\mathrm{per}}(t,\varepsilon)\,dt = c. \tag{1.9}$$

The system with the averaged coefficient will turn out to be a good approximation of the system with the rapidly oscillatory coefficient. In other words, the effect of rapidly periodic forcing is small.

1.7.2 Compartmentalization

Rapid fluctuation of the vertical swimming from the lower to the upper layer turns out to be negligible. However, rapid external fluctuation should also have an influence on a change of relative positions of cells, as in Figure 1.7.

To describe the dynamics of cells including changes of relative positions, we will introduce the idea of **compartmentalization**, as in compartmental models in epidemiology [BvdDW08].

Consider two schematic boxes; one for cells facing vertical, the other for cells facing horizontal as in Figure 1.7. Then consider dynamics within each box, as well as interactions between the two boxes. In other words, consider the densities of cells in the upper layer facing vertical u_1, those facing horizontal u_2, and likewise the density of cells in the lower layer facing vertical v_1, those facing horizontal v_2, as in Figure 1.8.

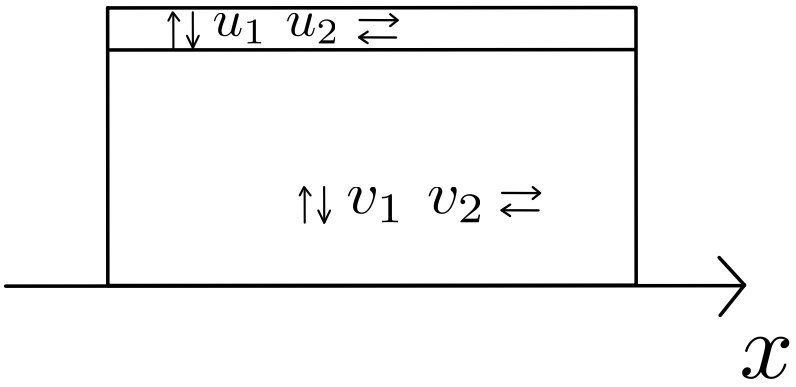

Figure 1.8: Compartmentalization. We consider cells in the upper layer facing vertical u_1, those facing horizontal u_2, cells in the lower layer facing vertical v_1, and those facing horizontal v_2.

We will study the exchange of the densities using the following matrix:

$$\begin{array}{c} \\ u_1 \\ u_2 \\ v_1 \\ v_2 \end{array} \begin{array}{c} \begin{array}{cccc} u_1 & u_2 & v_1 & v_2 \end{array} \\ \begin{pmatrix} -a & b & c & 0 \\ a & -b & 0 & 0 \\ 0 & 0 & -a-c & b \\ 0 & 0 & a & -b \end{pmatrix} \end{array} =: H. \tag{1.10}$$

This matrix tells us which variable loses or gains density, proportional to which rate.

For example, the $(1,1)$-entry and $(2,1)$-entry of the matrix H (1.10) tell us that

- the variable u_1 loses its density proportional to a positive coefficient a; and
- the variable u_2 gains the density the variable u_1 loses.

This exchange of density corresponds to the situation that a cell in the upper layer makes a change of direction from vertical position to horizontal position.

Similarly, the $(1,2)$-entry and $(2,2)$-entry of the matrix (1.10) tell us that

- the variable u_2 loses some of its density proportional to a coefficient b; and
- the variable u_1 gains the exactly the same density the variable u_2 loses.

This exchange of density corresponds to the situation that a cell in the upper layer makes a change of direction from horizontal position to vertical position.

The $(1,3)$-entry and the $(3,3)$-entry tell us that

- the variable v_1 loses some of its density proportional to a coefficient c; and

- the variable u_1 gains the exactly the same density the variable v_1 loses.

We assume that only cells in the lower layer that are facing vertical may arrive at the upper layer and stay vertical.

For the $(3,3)$-entry and the $(4,3)$-entry, as well as the $(3,4)$-entry and the $(4,4)$-entry, we assume the same responses as in the upper layer.

We assume diffusion of every variable following the Suematsu model, and we also assume that diffusion rates in the upper layer are much higher than diffusion rates in the lower layer.

For sinking due to gravity, we need a slight extension of the term in the Suematsu model to deal with four variables instead of two. We assume that both variables in the upper layer sink by the rate

$$\alpha(u_1 + u_2 + v_1 + v_2)^\beta \tag{1.11}$$

with some coefficients α and β. Here, using these coefficients α and β, we want to approximate some function depending on the sum of the densities. Moreover, we assume that sinking is relevant for both variables in the lower layer as cells may change the direction while sinking. We assume that sinking is governed by the following matrix:

$$\begin{array}{c} \\ u_1 \\ u_2 \\ v_1 \\ v_2 \end{array} \begin{array}{c} \begin{array}{cccc} u_1 & u_2 & v_1 & v_2 \end{array} \\ \begin{pmatrix} -1 & 0 & 0 & 0 \\ 0 & -1 & 0 & 0 \\ r_1 & r_2 & 0 & 0 \\ 1-r_1 & 1-r_2 & 0 & 0 \end{pmatrix} \end{array} =: G. \tag{1.12}$$

By the ratios $0 \le r_1 \le 1$ and $1 - r_1$, initially vertically facing cells u_1 change the direction while sinking and become either v_1 or v_2, and by the ratios $0 \le r_2 \le 1$ and $1 - r_2$, initially horizontally facing cells u_2 change the direction while sinking and become either v_1 or v_2. In terms of the resistance while sinking, the vertical direction should be more efficient than the horizontal direction, and we expect that both ratios $0 \le r_1 \le 1$ and $0 \le r_2 \le 1$ are near 1.

1.8 Analysis

Our new model will be a system of reaction-diffusion equations with four variables that captures also the change of direction of the cells. Let $\mathbf{u} = (u_1, u_2, v_1, v_2)^\intercal$, where the symbol $^\intercal$ denotes the transpose. Let $D = \mathrm{diag}(d_{11}, d_{12}, d_{21}, d_{22})$, and H and G be defined by (1.10), and (1.12) respectively.

$$\partial_t \mathbf{u} = D\Delta\mathbf{u} + \alpha(u_1 + u_2 + v_1 + v_2)^\beta G\mathbf{u} + H\mathbf{u}, \tag{1.13}$$

with Neumann boundary conditions. We assume that the power of sinking rate $\beta > 1$, the rates of changing direction while sinking $0 \le r_1, r_2 \le 1$, and all other constants $a, b, c, \alpha, d_{11}, d_{12}, d_{21}, d_{22} > 0$ are positive.

We will find a mathematical structure for pattern formation. Coefficients corresponding to stationary illumination, namely the case $a \ll b$ will turn out to induce

Turing instability. Moreover, we can characterize rapidly periodic illumination, by $a \approx b$, and letting a approach b can be interpreted as changing the illumination condition from stationary to rapidly periodic.

We may interpret the result as follows: Given a set of coefficients inducing Turing instability, increasing the tendency of making a change from vertical to horizontal directions, i.e. increasing a, corresponds to confusion of cells due to the external manipulation of the environment, and the system loses Turing instability, which explains non-pattern formation under periodic illumination.

1.9 Outline

The gist of the thesis is already presented in the introduction. The main contribution of this thesis is twofold: First, we provide a new biological hypothesis about the mechanism of negative phototaxis. Second, we extend an existing model to another that reveals more about the phenomenon, and provide an answer to a biological problem, backed up with mathematical structure. The resulting system looks like a standard reaction-diffusion equations and analysis then only requires well-known Turing instability analysis. However, our autonomous reaction-diffusion model of the time-periodic nonautonomous phenomenon is derived from an observation that the governing rules of the responses are time-independent. Our new model captures the essence of the phenomenon; the mechanism of negative phototaxis. Our analysis is mathematical evidence of our biological hypothesis (1.7).

The rest of the thesis is organized as follows: In Chapter 2, we will prove that the Suematsu model (1.1) without the nonlocal term has Turing instability.

In Chapter 3, we will replace one of the coefficients in the Suematsu model to discuss the behavior of solutions under rapidly periodic forcing. Applying the time-averaging theorem in [Mat08], we will show that the effect of rapidly periodic forcing is limited, and rapid fluctuation of the rate of vertical swimming is negligible.

In Chapter 4, we will derive and analyze our new compartmental model for both stationary and periodic illumination conditions. We will prove that the system has Turing instability for coefficients corresponding to stationary illumination and does not have Turing instability for coefficients corresponding to rapidly periodic illumination.

In Chapter 5, we will interpret the result and conclude with the future directions.

The table below (Table 1.1) summarizes the results obtained.

Illumination	stationary	periodic	stationary or periodic
Modeling	Suematsu et. al. [SAI$^+$11]	this thesis	this thesis
Analysis	Theorem 2.2.2	Theorem 3.3.1	Theorem 4.2.2
Pattern	Yes	Yes	Yes or No

Table 1.1: Comparison of the theorems

Chapter 2

Stationary illumination

This chapter is organized as follows: Section 1 introduces the concept of Turing instability. Section 2 presents the main theorem of this chapter. We prove that the Suematsu model (1.1) without the nonlocal term has Turing instability. Therefore, bioconvection patterns under stationary illumination can be explained by Turing instability. Section 3 deals with an invariant set for the Suematsu model (1.1) without the nonlocal term.

2.1 Turing instability

In the seminal paper on morphogenesis [Tur52], Turing showed that an originally quite homogeneous system may develop a pattern or structure due to an instability of the homogeneous equilibrium, which is triggered off by random disturbances.

Let

$$\mathbf{u} = \begin{pmatrix} u_1 \\ u_2 \\ \vdots \\ u_m \end{pmatrix}, \quad \mathbf{f}(\mathbf{u}) = \begin{pmatrix} f_1(u_1, u_2, \ldots, u_m) \\ f_2(u_1, u_2, \ldots, u_m) \\ \vdots \\ f_m(u_1, u_2, \ldots, u_m) \end{pmatrix},$$

and $D = \mathrm{diag}(d_1, d_2, \ldots, d_m)$. Consider a system of reaction-diffusion equations

$$\partial_t \mathbf{u} = D\Delta\mathbf{u} + \mathbf{f}(\mathbf{u}), \tag{2.1}$$

with Neumann boundary conditions, where $t > 0$, $\Omega \subset \mathbb{R}^n$, and Δ denotes the Laplace operator, i.e. $\Delta u_i = \sum_{i=1}^{n} \partial_{x_i}^2 u_i(x,t)$, where $i = 1, 2, \ldots, m$.

Remark. For the general framework of semilinear parabolic equations, we refer to [Hen81].

We refer to [Yan15] for existence and uniqueness of solutions of reaction-diffusion equations. For instance, assume that the initial conditions $u(x,0) = u_0(x)$ are continuous and f is of class C^1. Then, for any $t > 0$, there exists a unique smooth solution (of class C^1 with respect to $t > 0$; and of class C^2 with respect to $x \in \Omega$).

Definition 2.1.1. A system of ordinary differential equations

$$\partial_t \mathbf{u} = \mathbf{f}(\mathbf{u}) \tag{2.2}$$

is called the *kinetic system* of the system (2.1).

Definition 2.1.2. We call an equilibrium $\bar{\mathbf{u}}$ of the system (2.1) a *homogeneous equilibrium* if it is an equilibrium of the kinetic system, i.e.

$$\mathbf{f}(\bar{\mathbf{u}}) = 0. \tag{2.3}$$

Definition 2.1.3. We say a system of reaction-diffusion equations (2.1) has *Turing instability* if the system possesses an unstable homogeneous equilibrium which is stable in the kinetic system (2.2).

If a system has Turing instability, an originally homogeneous initial condition may evolve to a spatially nonconstant solution, which is triggered off by spatial disturbances. We are interested in such a solution and call it a *pattern*.

In [Per15], history of research on Turing instability is mentioned as follows: The first numerical simulations of a system exhibiting Turing patterns was published in 1972 involving the celebrated system of Gierer and Meinhardt [GM72]; it was only 20 years later that the first experimental evidence for a chemical reaction exhibiting spatial patterns explained by these principles was obtained and named the CIMA reaction, named after the name of the reactants used by P. De Kepper et al. [KCDB91] and Castets et al. [CDBDK90]; in 1995, S. Kondo and R. Asai [KA95] found an explanation of the patterns arising during the development of animals, proposing that the model should be set in a growing domain, opening up a larger class of possible patterns; and meanwhile several nonlinear parabolic systems exhibiting Turing patterns have been studied. Turing's mechanism is the simplest explanation for pattern formation and one of the most counter-intuitive results in the field of partial differential equations.

We refer to a two-volume-textbook on mathematical biology [Mur02] and [Mur03] which treats various biological problems accessible by mathematical analysis, in particular by Turing instability analysis.

A two-component reaction-diffusion system with conservation of mass was proposed as a model of cell polarity and analyzed in [IOM07], [OIC+07]. Turing instability analysis of a system with conservation of mass, in refined modern language, can be found in [MO10]. Written in Japanese, [Oga10] deals with bifurcation analysis of pattern dynamics of dissipative systems, and contains Turing instability analysis.

2.2 First theorem

Consider the Suematsu system (1.1) without the nonlocal term:

$$\begin{aligned} \partial_t u &= d_1 \Delta u - \alpha(u+v)^\beta u + cv =: d_1 \Delta u + f_1(u,v) \\ \partial_t v &= d_2 \Delta v + \alpha(u+v)^\beta u - cv =: d_2 \Delta v + f_2(u,v), \end{aligned} \tag{2.4}$$

where $x \in \Omega = [0, L] \subset \mathbb{R}$ and $t > 0$, with continuous initial conditions

$$\begin{aligned} u_0(x) &= u(x,0) \\ v_0(x) &= v(x,0) \end{aligned} \tag{2.5}$$

and Neumann boundary conditions

$$\partial_x u(t,0) = \partial_x u(t,L) = \partial_x v(t,0) = \partial_x v(t,L) = 0. \tag{2.6}$$

Assume that the power

$$\beta > 1, \tag{2.7}$$

and all other coefficients are positive, i.e.

$$c, \alpha, d_1, d_2, L > 0. \tag{2.8}$$

Lemma 2.2.1. *Consider the system (2.4), with initial conditions (2.5) and Neumann boundary conditions (2.6). Then, the averaged total mass*

$$s := \frac{1}{|\Omega|} \int_\Omega [u(x,t) + v(x,t)]\, dx \tag{2.9}$$

is conserved for any $t \geq 0$.

Proof. Summing up the two equations of the system (2.4), we have that the sum of the time derivatives equals the sum of diffusion and reaction terms. Moreover,

$$|\Omega| \frac{d}{dt} s = \frac{d}{dt} \int_\Omega [u(x,t) + v(x,t)]\, dx = \int_\Omega (d_1 \Delta u + d_2 \Delta v)\, dx = 0, \tag{2.10}$$

using the Green's formula and the Neumann boundary conditions. Therefore,

$$s = \frac{1}{|\Omega|} \int_\Omega (u(x,t) + v(x,t))\, dx \tag{2.11}$$

is a conserved quantity for any $t \geq 0$. □

Theorem 2.2.2. *Consider the system (2.4), with initial conditions (2.5), Neumann boundary conditions (2.6), the power condition (2.7), and the positivity condition (2.8). Then, there exists a unique positive homogeneous equilibrium*

$$\begin{pmatrix} \bar{u} \\ \bar{v} \end{pmatrix} = \begin{pmatrix} cs/(\alpha s^\beta + c) \\ s - cs/(\alpha s^\beta + c) \end{pmatrix}, \tag{2.12}$$

parametrized by any $s > 0$. Moreover, the homogeneous equilibrium (2.12) is stable in the kinetic system of the system (2.4). Assume

$$d_1 \partial_v f_1(\bar{u}, \bar{v}) - d_2 \partial_u f_1(\bar{u}, \bar{v}) \geq d_1 d_2. \tag{2.13}$$

Then the system (2.4) has Turing instability, i.e. the homogeneous equilibrium (2.12) loses the stability due to diffusion.

Proof. In (Step 1), we compute the homogeneous equilibrium using the conserved quantity (2.9).

In (Step 2), we eliminate the trivial eigenvalue 0 using the constraint of mass and study the linear stability of the homogeneous equilibrium under homogeneous perturbations. In (Step 3), we study the linear stability of the homogeneous equilibrium under nonhomogeneous perturbations.

(Step 1) Consider the homogeneous equilibrium $(\bar{u}, \bar{v})^\intercal$ of the system (2.4). Then the conserved quantity (2.9) satisfies

$$s := \frac{1}{|\Omega|} \int_\Omega [u(x,t) + v(x,t)]\, dx = \bar{u} + \bar{v}, \tag{2.14}$$

and hence

$$0 = -\alpha(\bar{u} + \bar{v})^\beta \bar{u} + c\bar{v} = -\alpha s^\beta \bar{u} + c(s - \bar{u}) = (-\alpha s^\beta - c)\bar{u} + cs. \tag{2.15}$$

By the power condition (2.7) and the positivity condition (2.8), we have

$$-\alpha s^\beta - c < 0. \tag{2.16}$$

Thus, we obtain

$$\begin{pmatrix} \bar{u} \\ \bar{v} \end{pmatrix} = \begin{pmatrix} cs/(\alpha s^\beta + c) \\ s - cs/(\alpha s^\beta + c) \end{pmatrix}.$$

(Step 2) Since

$$f_1 + f_2 = 0, \tag{2.17}$$

if we consider the stability of the homogeneous equilibrium (2.12) in the kinetic system of the system (2.4), we obtain a trivial eigenvalue 0 associated with the eigenvector

$$\begin{pmatrix} 1 \\ 1 \end{pmatrix}. \tag{2.18}$$

The eigenvalue 0 can be eliminated, if the mass s is fixed. We reduce the number of components by the constraint of mass (2.14), and consider the linear stability of the homogeneous equilibrium (2.12) in the kinetic system of the system (2.4), under the constraint of mass (2.14).

For any fixed $s > 0$, we have

$$\partial_t u = -\alpha(u + v)^\beta u + cv = -\alpha s^\beta u + c(s - u) = (-\alpha s^\beta - c)u + cs, \tag{2.19}$$

where

$$-\alpha s^\beta - c < 0, \tag{2.20}$$

by the power condition (2.7) and the the positivity condition (2.8). Notice that $u \to \bar{u}$ as $t \to \infty$ implies that $v = s - u \to s - \bar{u} = \bar{v}$ as $t \to \infty$ under the constraint of mass (2.14). Therefore, $(\bar{u}, \bar{v})^\intercal$ is asymptotically stable in the kinetic system of the system (2.4), under the constraint of mass (2.14).

(Step 3) Consider the full system (2.4) and linearize it about the homogeneous equilibrium (2.12). Equivalently, setting

$$w(x,t) = \begin{pmatrix} u(x,t) - \bar{u} \\ v(x,t) - \bar{v} \end{pmatrix}, \quad D := \operatorname{diag}(d_1, d_2), \quad f := \begin{pmatrix} f_1 \\ -f_1 \end{pmatrix}, \tag{2.21}$$

we linearize the system

$$\partial_t w = D\Delta w + f(w) \tag{2.22}$$

about the origin $w = (0,0)^\intercal$. We obtain

$$\partial_t w = D\Delta w + \mathbf{J}_2(\bar{u}, \bar{v})w, \tag{2.23}$$

where $\mathbf{J}_2$ denotes the Jacobi matrix of $f = (f_1, -f_1)^\intercal$.

Let $W(x)$ be the time-independent solution of the spatial eigenvalue problem

$$-\Delta W = k^2 W, \tag{2.24}$$

with the Neumann boundary condition

$$(\mathbf{n} \cdot \nabla) \cdot W = 0, \tag{2.25}$$

for $x \in \partial\Omega$. Let $W_k(x)$ be the eigenfunction corresponding to the wave number

$$k = m\pi/L. \tag{2.26}$$

Assume that each $W_k(x)$ satisfies the Neumann boundary conditions

$$(\mathbf{n} \cdot \nabla) \cdot W_k(0) = (\mathbf{n} \cdot \nabla) \cdot W_k(L) = 0. \tag{2.27}$$

Consider the exponential Ansatz

$$w(x,t) = \sum_k c_k \exp(\lambda t) W_k(x) \tag{2.28}$$

to the system (2.22), where c_k is determined by a Fourier expansion of the initial conditions in terms of $W_k(x)$. Note that λ is the eigenvalue which determines temporal growth.

Substituting the exponential Ansatz (2.28) into the linearized system (2.23), we have

$$\lambda \sum_k c_k \exp(\lambda t) W_k(x) = D \sum_k c_k \exp(\lambda t) \Delta W_k(x) + \mathbf{J}_2(\bar{u}, \bar{v}) \sum_k c_k \exp(\lambda t) W_k(x),$$

and cancelling $\exp(\lambda t)$, we obtain, for each k,

$$\begin{aligned} \lambda W_k(x) &= D\Delta W_k(x) + \mathbf{J}_2(\bar{u}, \bar{v}) W_k(x) \\ &= -Dk^2 W_k(x) + \mathbf{J}_2(\bar{u}, \bar{v}) W_k(x). \end{aligned}$$

Hence, we have

$$\left(\lambda I - \mathbf{J}_2(\bar{u}, \bar{v}) + Dk^2\right) W_k(x) = 0. \tag{2.29}$$

We require nontrivial solutions for $W_k(x)$ and obtain the characteristic polynomial

$$\left|\lambda I - \mathbf{J}_2(\bar{u}, \bar{v}) + Dk^2\right| = 0. \tag{2.30}$$

In order for the homogeneous equilibrium (2.12) to be unstable to spatial disturbances, we need an eigenvalue $\lambda = \lambda(k)$ of the matrix

$$\begin{aligned} A_k &:= \mathbf{J}_2(\bar{u}, \bar{v}) - Dk^2 \\ &= \begin{pmatrix} -k^2 d_1 + \partial_u f_1 & \partial_v f_1 \\ -\partial_u f_1 & -k^2 d_2 - \partial_v f_1 \end{pmatrix} \end{aligned} \tag{2.31}$$

such that, for some $k \geq 1$, the eigenvalue has positive real part.

Since

$$\begin{aligned} \mathrm{tr} A_k &= -k^2(d_1 + d_2) + \mathrm{tr}\mathbf{J}_2(\bar{u}, \bar{v}) \\ &= -k^2(d_1 + d_2) - \frac{\alpha\beta c s^\beta}{\alpha s^\beta + c} - \alpha s^\beta - c - \frac{\alpha\beta c s^\beta}{\alpha s^\beta + c} \\ &= -k^2(d_1 + d_2) - \alpha s^\beta - c \\ &< 0, \end{aligned} \tag{2.32}$$

the k-th mode is unstable if

$$\det A_k < 0. \tag{2.33}$$

Indeed, if

$$d_1 \partial_v f_1(\bar{u}, \bar{v}) - d_2 \partial_u f_1(\bar{u}, \bar{v}) \geq d_1 d_2, \tag{2.34}$$

so that

$$k^* := \sqrt{\frac{\partial_v f_1(\bar{u}, \bar{v})}{d_2} - \frac{\partial_u f_1(\bar{u}, \bar{v})}{d_1}} \geq 1,$$

we have

$$\begin{aligned} \det A_k &= (-k^2 d_1 + \partial_u f_1)(-k^2 d_2 - \partial_v f_1) + \partial_u f_1 \partial_v f_1 \\ &= k^4 d_1 d_2 + \partial_v f_1 k^2 d_1 - \partial_u f_1 k^2 d_2 - \partial_u f_1 \partial_v f_1 + \partial_u f_1 \partial_v f_1 \\ &= k^2 \left\{ k^2 - \left(\frac{\partial_v f_1}{d_2} - \frac{\partial_u f_1}{d_1} \right) \right\} < 0, \end{aligned}$$

for $k \in (0, k^*)$. Hence, for some $k \geq 1$, the eigenvalue has positive real part, i.e. the homogeneous equilibrium (2.12) is unstable.

□

Remark. In (Step 3), we studied the linear stability of the wave number k. Substituting

$$w = \tilde{w} \exp(\lambda t + ikx), \tag{2.35}$$

into the system (2.22), we obtain the Jacobi matrix (2.31).

Remark. Note that $c_k := (\alpha_k, \beta_k)^\intercal$ is determined by the following decomposition in terms of the Fourier modes:

$$\begin{aligned}\dot{\alpha_k} &= -k^2 d_1 \alpha_k + \hat{f}_k \\ \dot{\beta_k} &= -k^2 d_2 \beta_k - \hat{f}_k,\end{aligned}$$

where $k \geq 0$ and $\hat{f}_k$ is the k-th Fourier coefficient of the first component f_1.

Suppress the index 1 and write f instead of f_1 in this remark.

Here, $\alpha_0 + \beta_0$ is independent of time t and we look for the solution satisfying $\alpha_0 + \beta_0 = 0$, because we are looking for the solution to the original system (2.4), under the constraint of mass. Therefore, consider

$$\begin{aligned}\dot{\alpha_k} &= -k^2 d_1 \alpha_k + \hat{f}_k, \quad k \geq 0 \\ \dot{\beta_k} &= -k^2 d_2 \beta_k - \hat{f}_k, \quad k > 0 \\ \beta_0 &= -\alpha_0.\end{aligned} \tag{2.36}$$

We take the Taylor expansion of f at $(\bar{u}, \bar{v})^\intercal$:

$$\begin{aligned}f(u,v) = f(\bar{u},\bar{v}) + f_u(u-\bar{u}) + f_v(v-\bar{v}) \\ + \frac{f_{uu}}{2}(u-\bar{u})^2 + f_{uv}(u-\bar{u})(v-\bar{v}) + \frac{f_{vv}}{2}(v-\bar{v})^2 + \mathcal{O}(3).\end{aligned}$$

Here all the derivatives, e.g. f_u, f_v, are evaluated at $(\bar{u}, \bar{v})^\intercal$. Now the 0-th order equation of (2.36) reads

$$\dot{\alpha_0} = \hat{f}_0 = f(\alpha_0, \beta_0) + f_u \alpha_0 + f_v \beta_0 + \mathcal{O}(2) = (f_u - f_v)\alpha_0 + \mathcal{O}(2)$$

and the equilibrium α_0 is asymptotically stable as

$$f_u - f_v = \mathrm{tr}\mathbf{J}_2(\bar{u}, \bar{v}) < 0.$$

The Jacobi matrix of the nonzero modes of (2.36) is, for each $k \in \mathbb{N}$,

$$A_k := \mathbf{J}_2(\bar{u}, \bar{v}) - k^2 D = \begin{pmatrix} -k^2 d_1 + f_u & f_v \\ -f_u & -k^2 d_2 - f_v \end{pmatrix}. \tag{2.37}$$

2.3 Saturation of linear instability

To show that our nonlinear terms prevent the unstable equilibrium from growing indefinitely, we will show that the system (2.4) possesses a set with the property that if the initial and boundary values of a solution to the system lie in such a set, then the values also lie in the set. We call such a set a positively invariant set. First, we look for a positively invariant set for the kinetic system.

Proposition 2.3.1. *The kinetic system of the system (2.4) possesses a positively invariant set*

$$K = \{(u,v) \in \mathbb{R}^2 \,|\, u \geq 0, v \geq 0, u + v \leq s\}. \tag{2.38}$$

Proof. We consider nullclines under the constraint of conservation of mass $s = u+v$. Here, the nullclines $\partial_t u = f_1 = 0$ and $\partial_t v = f_2 = -f_1 = 0$ coincide and give us a line of equilibrium.

Consider the region defined by

$$K = \{(u, v) \in \mathbb{R}^2 \,|\, u \geq 0, v \geq 0, u + v \leq s\}, \tag{2.39}$$

as in Figure 2.1.

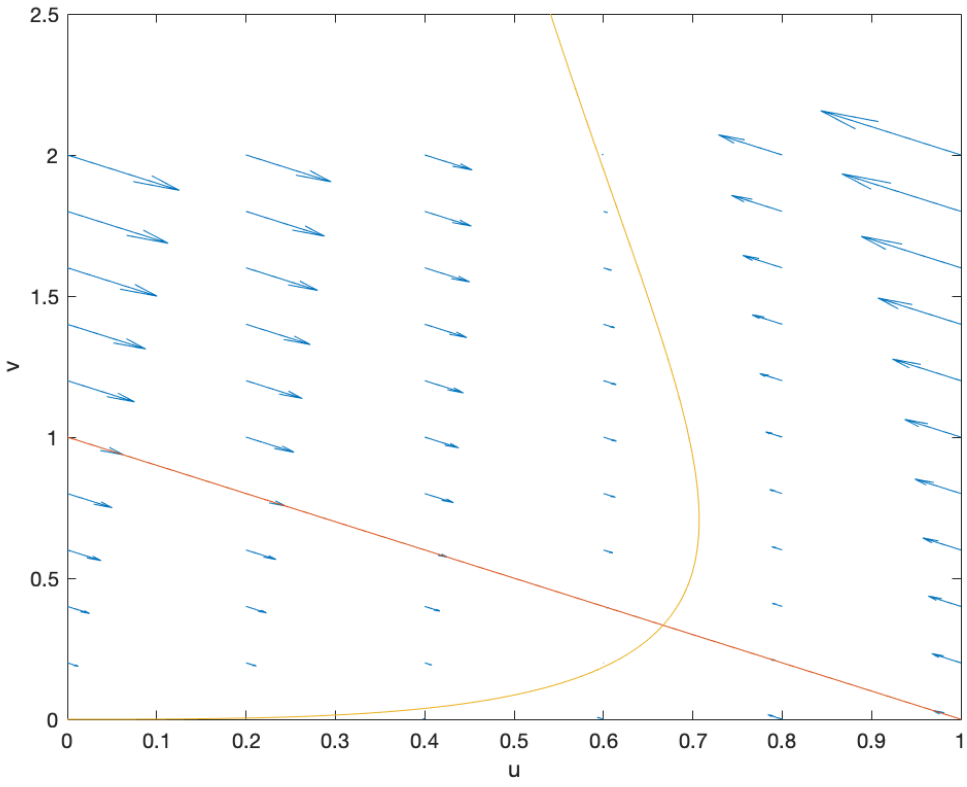

Figure 2.1: The set $K = \{(u, v) \in \mathbb{R}^2 \,|\, u \geq 0, v \geq 0, u + v \leq s\}$ is positively invariant for the kinetic system. Plot of vector field $(f_1, f_2) = (f_1, -f_1)^\intercal$ with coefficients $s = 1$, $c = 2$, $\alpha = 1$, and $\beta = 2$. Yellow line represents the line of equilibrium $f_1 = f_2 = 0$. Red line represents the constraint of mass $u + v = s$.

Then, on the u-axis, vectors within the triangle face upper left as the first component is negative and the second component is positive. On the v-axis, vectors within the triangle face lower right as the first component is positive and the second component is negative. On the line $u + v = s$, the equilibrium is asymptotically stable as we saw in (Step 2) of the proof of Theorem 2.2.2.

□

A triangular region, however, is not known to be positively invariant for a reaction-diffusion system with distinct diffusion rates. Therefore, we make a detour and take a family of rectangles inside the triangle, which evolves to the rectangle touching the stable equilibrium.

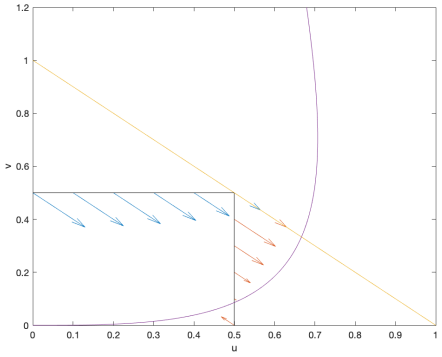

Figure 2.2: Illustration of vector field on the boundary when the rectangular region is off to the left.

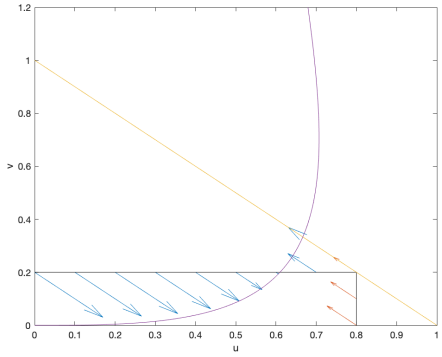

Figure 2.3: Illustration of vector field on the boundary when the rectangular region is off to the right.

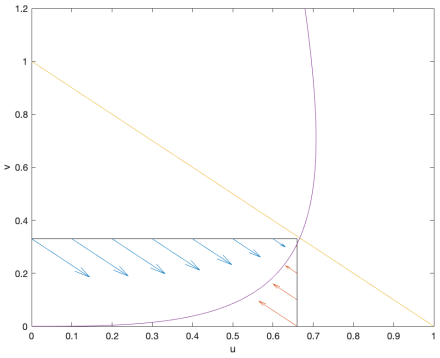

Figure 2.4: Illustration of vector field on the boundary when the rectangular region touches the intersection of the line of equilibrium and the constraint of mass.

Consider an extended system of the system (2.4):

$$\begin{aligned} \partial_t u &= d_1 \Delta u - \alpha(u+v)^\beta u + cv =: d_1 \Delta u + f_1(u,v) \\ \partial_t v &= d_2 \Delta v + \alpha(u+v)^\beta u - cv =: d_2 \Delta v + f_2(u,v) \\ \dot{t} &= 1, \end{aligned} \tag{2.40}$$

and denote the nonlinearity of this extended system by

$$F(u_1, u_2, v_1, v_2) = \begin{pmatrix} f_1(u, v) \\ f_2(u, v) \\ 1 \end{pmatrix}. \tag{2.41}$$

Define

$$S := \{(u, v, t) \,|\, (u, v) \in \Gamma(t), t \geq 0\}. \tag{2.42}$$

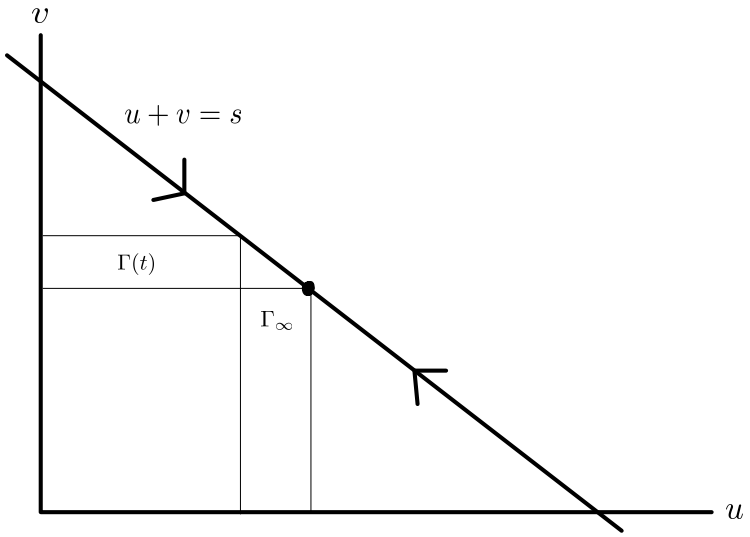

Figure 2.5: Cross-section of the invariant set $\Gamma(t)$ converges to Γ_∞.

Proposition 2.3.2. *The set S is positively invariant for the extended system (2.40).*

Proof. We will show that for the outward normal η at any boundary point $\mathbf{u}_* \in \partial\Gamma(t)$, the inner product is negative, i.e.

$$\langle \eta, F(\mathbf{u}_*, \mathbf{t}) \rangle \leq 0, \tag{2.43}$$

for $(x, t) \in \Omega \times (0, T]$. Then a corollary to Theorem 1 in [Wei75] shows that S is a positively invariant set. Theorem 1 in [Wei75] assumes that diffusion coefficients are equal, but we have two distinct diffusion coefficients $d_1 \neq d_2$. However, the normal vector of the boundary of a rectangle whose edges are parallel to the axes has 0 as one of the first two components. Hence, multiplying the nonlinearity (2.41) by such a normal vector, only one of the two diffusion coefficients appears in an inequality. Therefore, Theorem 1 in [Wei75] is applicable, and a corollary reads as follows:

Lemma 2.3.3. *[Wei75] Let S be a closed convex subset of $\mathbb{R}^m$ with the property that for any outward normal at any boundary point of S, the inequality (2.43) is satisfied. Here, m denotes the number of components of the extended system.*

Assume that the nonlinearity (2.41) is uniformly Hölder continuous in x and t and Lipschitz continuous in $(u, v, t)^\intercal$ for $(x, t) \in \Omega \times (0, T]$.

If $(u, v, t)^\intercal$ is any solution of the extended system in $(x, t) \in \Omega \times (0, T]$ which is continuous in $(x, t) \in \bar{\Omega} \times (0, T]$, and if the values of $(u, v, t)^\intercal$ on $\bar{\Omega} \times \{0\}$ and on $\partial\Omega \times [0, T]$ are bounded and Hölder continuous and lie in S, then $(u, v, t)^\intercal \in S$ in $\Omega \times (0, T]$.

To apply Lemma 2.3.3, we compute the inner product.

Imagine S as a cuboid whose bottom lies on $\Gamma(0)$ and evolves in the time-direction. The right vertical edge of the bottom evolves in the time direction, constituting a sidewall of the boundary of M. Similarly, the upper horizontal edge evolves in the time direction, constituting another sidewall. Two sides of S are flat because the u-axis and v-axis do not evolve over time, and the cross-section $\Gamma(t)$ converges to Γ_∞ as $t \to \infty$.

Let h_1 be the first component of the flux vector on the sidewall of the right vertical edge of $\Gamma(t)$.

$$h_1 = \langle \eta, \partial_t (u, v, t)^\intercal \rangle, \tag{2.44}$$

where η is the outer normal vector on the boundary of M.

On the sidewall of the right vertical edge, the outer normal is $\eta = (1, 0, f_1(\mathbf{u}_*))^\intercal$, and

$$h_1 = d_1 \Delta u + f_1(\mathbf{u}_*). \tag{2.45}$$

Similarly, let h_2 be the second component of the flux vector on the sidewall of the side wall of the upper horizontal edge of $\Gamma(t)$.

$$h_2 = \langle \eta, \partial_t (u, v, t)^\intercal \rangle. \tag{2.46}$$

Similarly, on the upper horizontal edge, the outer normal vector is $\eta = (0, 1, f_2(\mathbf{u}_*))^\intercal$ and

$$h_2 = d_2 \Delta v + f_2(\mathbf{u}_*). \tag{2.47}$$

If we have both

$$h_1, h_2 \leq 0, \tag{2.48}$$

then we have an inward flux on the boundary of S.

Now, on the vertical edge of the cross-section Γ_∞, we have monotonicity in v. That is,

$$\partial_v f_1 = c - \alpha\beta(u + v)^{\beta - 1} u \geq c - \alpha\beta s^\beta \tag{2.49}$$

and if

$$c - \alpha\beta s^\beta \geq 0, \tag{2.50}$$

we have

$$\partial_v f_1 \geq 0. \tag{2.51}$$

If

$$\partial_v f_1 = c - \alpha\beta(u_* + v)^{\beta - 1} u_* \leq c - \alpha\beta u_*^\beta \leq 0, \tag{2.52}$$

we have

$$\partial_v f_1 \leq 0. \tag{2.53}$$

For either case, we have a non-positive value of f_1 as

$$f_1(u_*, v_*) = 0 \leq 0, \tag{2.54}$$

and

$$f_1(u_*, 0) = -\alpha u_*^{\beta+1} \leq 0. \tag{2.55}$$

Similarly, on the horizontal edge of the cross-section Γ_∞, we have monotonicity in u:

$$\partial_u f_2 = \alpha\beta u(u+v)^{\beta-1} + \alpha(u+v)^\beta \geq 0, \tag{2.56}$$

and

$$\partial_u f_2 \geq 0. \tag{2.57}$$

At the corner, we have

$$f_2(u_*, v_*) = 0 \leq 0. \tag{2.58}$$

By the maximum principle, both Δu and Δv take the maximum value 0 at the boundary. Hence, we have both

$$h_1, h_2 \leq 0, \tag{2.59}$$

for $(x, t) \in \Omega \times (0, T]$.

□

Chapter 3

Effect of rapidly periodic forcing

This chapter is organized as follows: Section 1 introduces a rapidly periodic forcing

$$c_{\mathrm{per}}(t,\varepsilon) := c[1+\cos(2\pi t/\varepsilon)], \tag{3.1}$$

where $0 < \varepsilon \ll 1$. Section 2 introduces Gevrey regularity so that we can state the time-averaging theorem which we want to apply. Section 3 contains the main theorem of this chapter. To examine the effect of rapidly periodic forcing on the Suematsu model without the nonlocal term (2.4), we will apply a time-averaging theorem for semilinear parabolic partial differential equations under rapid quasi-periodic forcing [Mat08]. The system with the averaged intensity coefficient

$$\langle c_{\mathrm{per}}(t,\varepsilon)\rangle := \frac{1}{\varepsilon}\int_0^\varepsilon c_{\mathrm{per}}(t,\varepsilon)\,dt = \frac{1}{\varepsilon}\int_0^\varepsilon c[\cos(2\pi t/\varepsilon)+1]\,dt = c. \tag{3.2}$$

turns out to be a good approximation of the system with rapidly periodic forcing $c_{\mathrm{per}}(t,\varepsilon)$.

3.1 System with rapidly periodic forcing

We study the effect of rapidly periodic forcing of stationary illumination. Instead of taking a constant rate of exchange from the lower layer to the upper layer, we take a rapidly periodic coefficient

$$c_{\mathrm{per}}(t,\varepsilon) := c[1+\cos(2\pi t/\varepsilon)], \tag{3.3}$$

where $0 < \varepsilon \ll 1$. This coefficient is designed so that the averaged intensity corresponds to the stationary illumination.

Consider the Suematsu model with rapidly periodic forcing as follows:

$$\begin{aligned}
\partial_t u &= d_1\Delta u - \alpha(u+v)^\beta u + c_{\mathrm{per}}(t,\varepsilon)v \\
&= d_1\Delta u - \alpha(u+v)^\beta u + cv + c\cos(2\pi t/\varepsilon)v \\
&= d_1\Delta u - \alpha(u+v)^\beta u + cv + \frac{1}{\varepsilon}\int_0^\varepsilon c\cos(2\pi t/\varepsilon)v\,dt \\
&\qquad + c\cos(2\pi t/\varepsilon)v - \frac{1}{\varepsilon}\int_0^\varepsilon c\cos(2\pi t/\varepsilon)v\,dt \\
\partial_t v &= d_2\Delta v + \alpha(u+v)^\beta u - c_{\mathrm{per}}(t,\varepsilon)v \\
&= d_2\Delta v + \alpha(u+v)^\beta u - cv - c\cos(2\pi t/\varepsilon)v \\
&= d_2\Delta v + \alpha(u+v)^\beta u - cv - \frac{1}{\varepsilon}\int_0^\varepsilon c\cos(2\pi t/\varepsilon)v\,dt \\
&\qquad - c\cos(2\pi t/\varepsilon)v + \frac{1}{\varepsilon}\int_0^\varepsilon c\cos(2\pi t/\varepsilon)v\,dt,
\end{aligned} \tag{3.4}$$

where $0 < \varepsilon \ll 0$.

3.2 Time-averaging

We will apply theorem B on p.434 in [Mat08] to obtain an estimate of the effect of rapid forcing.

3.2.1 Gevrey regularity

Before stating assumptions for the time-averaging theorem, let us introduce some terminology.

We will follow [Mat01], which extended results of [FT98]. For the description of Sobolev spaces; see [Tem88].

Definition 3.2.1. Let $\Omega = [0, L]^d$, $d = 1, 2, 3$, where $L > 0$. Gevrey class $\mathcal{G}_{\sigma,\nu}(\Omega, \mathbb{R}^n)$ is defined by

$$\mathcal{G}_{\sigma,\nu}(\Omega, \mathbb{R}^n) := \mathcal{D}\left(A^\nu \exp(\sigma(-\Delta)^{1/2})\right), \tag{3.5}$$

where $A = -\operatorname{diag}(d_1, \ldots, d_n)\Delta$ is a sectorial operator.

A norm is given by

$$|u|_{\mathcal{G}_{\sigma,\nu}} = \left(\sum_{k=1}^n \sum_{j\in\mathbb{Z}^d} u_k^j u_k^j (1 + d_k\|j\|^2)^{2\nu} \exp(2\sigma\|j\|)\right)^{1/2}, \tag{3.6}$$

where d_k is the diffusion coefficient of the k-th component and u_k^j is the k-th component of the Fourier coefficient of the Fourier expansion of the periodic function u into $\exp(i\frac{2\pi}{L} j \cdot x)$.

Gevrey class $\mathcal{G}_{\sigma,\nu}(\Omega,\mathbb{R}^n)$ contains functions whose Fourier modes decay exponentially fast. For $\sigma > 0$, the Fourier coefficients u_j of $u \in \mathcal{G}_{\sigma,\nu}(\Omega,\mathbb{R}^n)$ decay like

$$\|j\|^{-2\nu} \exp(-\sigma\|j\|). \tag{3.7}$$

Gevrey class $\mathcal{G}_{\sigma,\nu}(\Omega,\mathbb{R}^n)$ is a Hilbert space with the scalar product

$$(v,w)_{\mathcal{G}_{0,\nu}} = \sum_{k=1}^{n} \sum_{j\in\mathbb{Z}^d} v_k^j w_k^j (1 + d_k\|j\|^2)^{2\nu} \exp(2\sigma\|j\|), \tag{3.8}$$

where v^j and w^j are the Fourier coefficients in $\mathbb{R}^n$ of the periodic functions v and w. Note that

$$\mathcal{G}_{0,\nu}(\Omega,\mathbb{R}^n) = H^{2\nu}_{\text{per}}(\Omega,\mathbb{R}^n) = X^\nu, \tag{3.9}$$

with $X = L^2(\Omega,\mathbb{R}^n)$.

By $H^m_{\text{per}}(\Omega)$, or also $W^{m,p}_{\text{per}}(\Omega)$, we denote the space of restrictions to Ω of periodic functions which are in $H^m(\mathcal{O})$, or $W^{m,p}(\mathcal{O})$, on every bounded open set $\mathcal{O}$. To study the spaces $H^m_{\text{per}}(\Omega)$, we can use the Fourier series expansion

$$u(x) = \sum_{j\in\mathbb{Z}^n} u_j \exp(i\frac{2\pi}{L} j\cdot x), \tag{3.10}$$

with $\bar{u_k} = u_{-k}$ so that u is real. Then u is in $L^2(\Omega)$ if and only if

$$\|u\|^2_{L^2(\Omega)} = |\Omega| \sum_{j\in\mathbb{Z}^n} |u_j|^2 < \infty, \tag{3.11}$$

and u is in $H^m_{\text{per}}(\Omega)$, $s \in \mathbb{R}_+$, if and only if

$$\sum_{j\in\mathbb{Z}^n} (1 + |j|^2)^s |u_j|^2 < \infty. \tag{3.12}$$

Lemma 3.2.1. *[Mat01] For $\nu > d$ and $\sigma > 0$, all functions $u \in \mathcal{G}_{\sigma,\nu}(\Omega,\mathbb{R}^n)$ are real analytic.*

3.2.2 Assumptions

Below, we will collect assumptions in the theorem.

(H1) There exists a sequence of Galerkin projections $(P_N)_{N\in\mathbb{N}}$ which satisfy the following:

(i) The sequence of projections converges strongly to the identity on X:

$$\lim_{N\to\infty} P_N u = u \tag{3.13}$$

in X for all $u \in X$.

(ii) The projections P_N commute with A on its domain of definition

$$P_N A u = A P_N u \tag{3.14}$$

for all $u \in \mathcal{D}(A)$.

(iii) The operator A is bounded on the range of P_N

$$|A P_N u|_X \leq N |P_N u|_X \tag{3.15}$$

for all $u \in X$.

(H2) In the periodic case $p = 1$, we require $\omega \neq 0$.

In the quasi-periodic case, let $\omega \in \mathbb{R}^p$ be such that there exist constants $\gamma > 0$ and $\tau > p - 1$ such that for all $m \in \mathbb{Z}^p \setminus \{0\}$,

$$|(m, \omega)| \geq \gamma |m|^{-\tau}, \tag{3.16}$$

where $(\cdot\,, \cdot)$ denotes the inner product on $\mathbb{R}^p$ and $|\cdot|$ denotes the norm of m, i.e. $|m| = \sum_{j=1}^{p} |m_j|$.

(H3) For all $\varepsilon > 0$ and $u \in X$ the quasi-periodic term has zero mean:

$$\int_{\theta \in \mathbb{T}} g(u, \theta, \varepsilon)\, d\theta = 0. \tag{3.17}$$

(H4) There exists a closed, densely defined, boundedly invertible operator $\Gamma_{\sigma,\nu}$ with the domain of definition

$$\mathcal{G}_{\sigma,\nu} := \mathcal{D}(\Gamma_{\sigma,\nu}) \subset \mathcal{D}(A) \tag{3.18}$$

such that $\mathcal{R}(P_N) \subset \mathcal{G}_{\sigma,\nu}$, $\Gamma_{\sigma,\nu}(\mathcal{R}(P_N)) = \mathcal{R}(P_N)$ for all N, and $\Gamma_{\sigma,\nu} A u = A \Gamma_{\sigma,\nu} u$ for all $u \in \mathcal{R}(P_N)$. Here by $\mathcal{D}$ and $\mathcal{R}$, we denote the domain, and the range, respectively. We equip the Gevrey spaces $\mathcal{G}_{\sigma,\nu}$ with the graph norm

$$|u|_{\mathcal{G}_{\sigma,\nu}} = |u|_X + |\Gamma_{\sigma,\nu} u|_X. \tag{3.19}$$

We assume that Gevrey-smooth functions are exponentially well approximated by the Galerkin projections P_N

$$|\Gamma_{\sigma,\nu}^{-1}(\mathrm{id} - P_N)|_{L(X,X)} \leq C_0 \exp(-\ell_0 / N^{\nu}) \tag{3.20}$$

for N-independent constants $C_0(\sigma, \nu)$ and $c_0(\sigma, \nu)$.

(H5) There is a Gevrey class $Y = \mathcal{G}_{\sigma,\nu}$ with $\sigma, \nu > 0$ and a constant $\delta > 0$ for the size of the complex extension such that the following properties of the nonlinearities hold.

The nonlinearities $f : (Y + \delta) \to Y_{\mathbb{C}}$ and $g : (Y + \delta) \times (\mathbb{T} + \delta) \times \mathbb{R} \to Y_{\mathbb{C}}$ are analytic and bounded on bounded subsets when considered on Gevrey spaces, extended in the complex direction. In addition, all of the above statements are assumed to hold when the space of Gevrey regularity $Y = \mathcal{G}_{\sigma,p}$ is replaced by $Y = X$.

(H6) The operator A generates a strongly continuous semigroup both on X and $\mathcal{G}_{\sigma,\nu}$.

3.2.3 Time-averaging theorem

The theorem to apply is on page 434 in [Mat08] which reads as follows:

Proposition 3.2.2. *[Mat08] Let X be a real Banach space and A be a closed densely defined operator with domain $\mathcal{D}(A)$ generating a strongly continuous semigroup. Denote by $\mathbb{T} = (\mathbb{R}/\mathbb{Z})^p$ the p-dimensional torus. Consider the following initial value problem on the phase space $X \times \mathbb{T}$:*

$$\dot{u} = Au + f(u) + g(u, \theta, \varepsilon) \tag{3.21}$$
$$\dot{\theta} = \omega/\varepsilon, \tag{3.22}$$

where $t > 0$, $u \in X$, $\theta \in \mathbb{T}$, and $0 < \varepsilon \ll 1$, with initial conditions $u(0) = u_0$ and $\theta(0) = \theta_0$. Assume (H1)-(H5), then for any ball of radius R in $\mathcal{G}_{\sigma,\nu}$, there exists an $\varepsilon_0 > 0$ such that for $0 < \varepsilon < \varepsilon_0$, the following holds: There exists a C^1-near-identity-transformations $u = v + \varepsilon w(v, \theta, \varepsilon)$ such that the transformed equation has the form

$$\dot{v} = Av + f(v) + \bar{g}(v, \varepsilon) + r(v, \theta, \varepsilon) \tag{3.23}$$
$$\dot{\theta} = \omega/\varepsilon, \tag{3.24}$$

with initial conditions $v(0) = u_0$ and $\theta(0) = \theta_0$, where $\bar{g}$ and r are some bounded functions on balls in X satisfying

$$|\bar{g}(v, \varepsilon)|_X \leq C(|v|_X)\varepsilon^{(\tau+1)/(\tau+1+1/\nu)} \tag{3.25}$$
$$|r(v, \theta, \varepsilon)|_X \leq C(|v|_{\mathcal{G}_{\sigma,\nu}}) \exp(-\ell/\varepsilon^{1/(\tau+1+1/\nu)}). \tag{3.26}$$

Assume also that (H6) holds. Then the solutions of the truncated equation

$$\dot{\bar{v}} = A\bar{v} + f(\bar{v}) + \bar{g}(\bar{v}, \varepsilon) \tag{3.27}$$
$$\dot{\theta} = \omega/\varepsilon, \tag{3.28}$$

with initial condition $\bar{v}(0) = u_0$ and $\theta(0) = \theta_0$ remain close to the solutions of the transformed equation (3.23), i.e.

$$|v(t) - \bar{v}(t)|_X \leq C(T, R) \exp(-\ell/\varepsilon^{1/(\tau+1+1/\nu)}), \tag{3.29}$$

for some $C(T, R)$ where $v(t)$ is a solution of the equation (3.23), resp. $\bar{v}(t)$ is a solution of the equation (3.27), that remains inside the ball $B_R(\mathcal{G}_{\sigma,\nu})$ for $t \in [0, T]$.

3.3 Second theorem

As an application of the time-averaging theorem, we can say that the effect of rapidly periodic forcing is negligible.

Theorem 3.3.1. *Consider the Suematsu model with rapidly periodic forcing (3.4). Then the effect of rapidly periodic forcing is exponentially small. More precisely, there exists a time-periodic coordinate transformation that converts the system (3.4) into the Suematsu model without the nonlocal term (2.4) with an exponentially small remainder which can be truncated without any qualitative change of behavior of solutions.*

Proof. Theorem 3.3.1 is a straightforward application of Proposition 3.2.2 to the system (3.4). To apply the proposition, We need to show that the conditions (H1)-(H6) are satisfied:

(H1) Projection to spatial Fourier modes satisfies the conditions.

(H2) Our forcing $c\cos(2\pi t/\varepsilon)$ is periodic and $1 = \omega \neq 0$.

(H3) For all ε and $(u, v)^\intercal \in X$ the periodic term has zero mean. In fact, we have subtracted the mean before so that this assumption is satisfied. We can explicitly check the condition as follows:

$$\begin{aligned}
&\int_0^1 \left[c\cos(2\pi t/\varepsilon)v(x,t) - \frac{1}{\varepsilon}\int_0^\varepsilon c\cos(2\pi t/\varepsilon)v(x,t)\,dt \right] d\theta \\
&= \int_0^1 \left[c\cos(2\pi\theta)v(x,\varepsilon\theta) - \int_0^1 c\cos(2\pi t')v(x,\varepsilon t')\,dt' \right] d\theta \\
&= \int_0^1 c\cos(2\pi\theta)v(x,\varepsilon\theta)\,d\theta - \int_0^1 c\cos(2\pi t')v(x,\varepsilon t')\,dt' \\
&= 0,
\end{aligned}$$

where $\theta := t/\varepsilon$.

(H4) The operator $\Gamma_{\sigma,\nu}$ is designed so that it behaves like $\exp(\sigma|A|^\nu)$.

For sectorial operators like the Laplacian $A = \Delta$ on regular domains, the Gevrey space can be defined as the domain of $\Gamma_{\sigma,\nu} = \exp(\sigma(-A)^\nu)$.

We may define the norm by

$$|u(t)|_{\mathcal{G}_{\sigma,1/2}} = |u|_X + |\exp(\sigma(-\Delta)^{1/2})u|_X. \tag{3.30}$$

The Gevrey norm can be expressed in spatial Fourier modes. For

$$u(x) = \sum_{k\in\mathbb{Z}} u_k \exp(i2\pi kx) \in \mathcal{G}_{\sigma,1/2}, \tag{3.31}$$

with $u_k \in \mathbb{C}^n$, we have

$$|u|^2_{\mathcal{G}_{\sigma,1/2}} = \sum_{k\in\mathbb{Z}} |u_k|^2(1+\exp(\sigma|k|))^2. \tag{3.32}$$

Let

$$P_N u = \sum_{k\in\mathbb{Z}, 4\pi^2|k|^2\leq N} u_k \exp(i2\pi kx). \tag{3.33}$$

Then

$$|(id - P_N)u|_X = \left| \sum_{k\in\mathbb{Z},|k|>\sqrt{N}} u_k \exp(i2\pi kx) \right|_X \leq \exp(-\sigma N^{1/2})|u|_{\mathcal{G}_{\sigma,1/2}}. \quad (3.34)$$

(H5) Our nonlinearity is entire in u and real analytic in θ, hence it is analytic in $\mathcal{G}_{\sigma,1/2}$ and in X.

(H6) In the case of reaction-diffusion equations, the sectorial operator $A = D\Delta$ generates a strongly continuous semigroup both on X and $\mathcal{G}_{\sigma,1/2}$.

By the Proposition 3.2.2, there exists a time-periodic coordinate transformation that converts the Suematsu model with rapidly periodic forcing (3.4) into the Suematsu model with correction and some remainder.

Moreover, the nonautonomous remainder is exponentially small, namely

$$|r(u,\theta,\varepsilon)|_X \leq C(|u|_{\mathcal{G}_{\sigma,1/2}}) \exp(-\ell/\varepsilon^{1/(\tau+3)}), \quad (3.35)$$

where $\nu = 1/2$, and the solutions to the truncated system, i.e. the Suematsu model with the averaged coefficient $\langle c_{\text{per}}(t,\varepsilon)\rangle = c$ and some correction, with relevant initial conditions remain close to the solutions to the system with the remainder, namely

$$|r(u(t),\theta(t),\varepsilon)|_X \leq C(|u_0|_X) \exp(-\ell(t)/\varepsilon^{1/(\tau+3)}), \quad (3.36)$$

with $\ell(t) = \min(t, t^*, \ell)$, where t^* is the maximal Gevrey exponent.

Finally, recall that we added and subtracted the mean of oscillation

$$\frac{1}{\varepsilon}\int_0^\varepsilon c\cos(2\pi t/\varepsilon)v(x,t)\,dt \quad (3.37)$$

for both components. Provided that ε is small, i.e. the oscillation is rapid, the variable v does not change much during the short time-interval, so that we can put it outside the integral, to approximate the value of the integral. But then,

$$\int_0^\varepsilon c\cos(2\pi t/\varepsilon)\,dt = 0, \quad (3.38)$$

and the mean turns out to be small. Thus the averaged system with correction approximates well the Suematsu model with rapidly periodic forcing.

□

Chapter 4

Stationary or rapidly periodic illumination

This chapter is organized as follows: In Section 1, we derive a new model using the idea of compartmentalization and time-averaging. The new model assumes the biological hypothesis (1.7); that is, Euglena gracilis makes a change of direction if it senses flicker.

The new compartmental model has Turing instability for coefficients corresponding to stationary illumination and loses Turing instability for coefficients corresponding to rapidly periodic illumination. Therefore, the failure of pattern formation under certain rapidly periodic illumination can be explained by the loss of Turing instability.

4.1 Modeling

Negative phototaxis is directional. To understand the mechanism of negative phototaxis, we distinguish cells between those facing perpendicular to the light source and those facing parallel to the light source.

Different responses depending on the relative positions of cells boil down to a simple single rule (1.7). Based on this rule, we build a new model not only for stationary illumination but also for rapidly periodic illumination.

4.1.1 Compartmentalization

Let u_1, u_2, v_1, and v_2 denote the density of cells in the upper layer facing vertical, that of those facing horizontal, the density of cells in the lower layer facing vertical, and that of those facing horizontal, respectively. We will then describe the exchange of densities using the following matrix:

$$\begin{array}{c} \\ u_1 \\ u_2 \\ v_1 \\ v_2 \end{array} \begin{array}{c} \begin{array}{cccc} u_1 & u_2 & v_1 & v_2 \end{array} \\ \begin{pmatrix} -a & b & c_{\mathrm{per}}(t,\varepsilon) & 0 \\ a & -b & 0 & 0 \\ 0 & 0 & -a-c_{\mathrm{per}}(t,\varepsilon) & b \\ 0 & 0 & a & -b \end{pmatrix} \end{array} \tag{4.1}$$

Here, we assumed the same responses both in the upper and the lower layers but assumed that only cells in the lower layer that are facing vertical may arrive at the upper layer remaining to be vertical.

Observe that the frequency of periodic shading due to the rotation, which is of order of seconds, is rapid, in the time-scale of pattern formation, which is of order of 10 minutes. Moreover, Theorem 3.3.1 guarantees that rapid external forcing by $c_{\mathrm{per}}(t,\varepsilon) := c[1+\cos(2\pi t/\varepsilon)]$ is qualitatively equivalent to stationary illumination by

$$\langle c_{\mathrm{per}}(t,\varepsilon)\rangle := \frac{1}{\varepsilon}\int_0^\varepsilon c[1+\cos(2\pi t/\varepsilon)]\,dt = c.$$

In other words, the oscillatory illumination from below is so rapid that only the averaged amount of light matters to drive cells to swim away. On the other hand, rapidly periodic forcing causes a change of direction of cells. Thus, the cells in the lower layer that are facing vertical may swim away vertically, but some cells make a change of direction because their sensors receive periodic light, remaining in the lower layer, facing the other direction.

Averaging out the rapidly periodic coefficient $c_{\mathrm{per}}(t,\varepsilon) = c$ in the compartmentalization matrix (4.1), we obtain the compartmentalization matrix H defined in (1.10).

4.1.2 Characterization of illumination conditions

Now, we characterize illumination conditions by different responses depending on the relative position.

First, consider stationary illumination from below. (Assume that illumination is strong enough to induce negative phototaxis.)

- If a cell faces vertical relative to the planar light source, then it senses **stationary light input**, as in Figure 1.7.
- On the other hand, if a cell faces horizontal relative to the source, then it senses **periodic light input**, due to its own rotation with frequency about 1 Hz.

Next, consider rapidly periodic illumination from below of period same as the intrinsic rotation with frequency about 1 Hz. (Assume again that the averaged intensity is high enough to induce negative phototaxis.)

- If a cell faces vertical relative to the planar light source, then it senses **periodic light input**, due to external oscillation as in Figure 1.7.
- On the other hand, if a cell faces horizontal relative to the source, then it also senses **periodic light input**, due to both its own rotation and external oscillation. Here the period of light input depends on the two phases of oscillations, but we focus on its periodicity and ignore fluctuations of the period of light input.

We suppose that phototaxis, including negative phototaxis, is optimized in stationary illumination as it should cause a cell to swim to a more preferable environment and we will formulate negative phototaxis as follows: A cell behaves according to the input its sensor receives.

- If its sensor receives stationary input, then the cell keeps the direction, as the present direction is already good. Here, we do not distinguish between cases a cell faces toward and away from the light source.
- If its sensor receives periodic input, then the cell makes a change of direction, as the present direction is not good for it to get away from light. Here, it is possible that as a result of the turn, it ends up facing toward the light source.

Different responses depending on the relative positions boil down to a single rule: **Euglena gracilis makes a change of direction if it senses flicker** of frequency $\approx$ 1Hz of its intrinsic rotation.

Therefore, we may characterize illumination conditions by coefficients in the compartmentalization matrix H defined by (1.10) as follows:

- Stationary illumination corresponds to the case where vertical cells tend to keep vertical and horizontal cells tend to make a change of direction, i.e. $a \ll b$.
- rapidly periodic illumination corresponds to the case where both vertical cells and horizontal cells equally tend to make a change of direction, i.e. $a \approx b$.

See Figure 4.1.

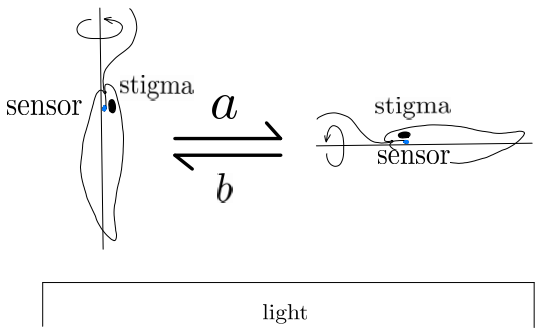

Figure 4.1: The tendency of making a change of direction from vertical to horizontal relative position a; and the tendency of making a change of direction from horizontal to vertical relative position b.

4.1.3 New model

Let $\mathbf{u} := (u_1, u_2, v_1, v_2)^\intercal$, $\mathbf{f} := (f_1, f_2, f_3, f_4)^\intercal$, $D := \operatorname{diag}(d_{11}, d_{12}, d_{21}, d_{22})$,

$$G := \begin{pmatrix} -1 & 0 & 0 & 0 \\ 0 & -1 & 0 & 0 \\ r_1 & r_2 & 0 & 0 \\ 1-r_1 & 1-r_2 & 0 & 0 \end{pmatrix}, \quad \text{and} \quad H := \begin{pmatrix} -a & b & c & 0 \\ a & -b & 0 & 0 \\ 0 & 0 & -a-c & b \\ 0 & 0 & a & -b \end{pmatrix}.$$

We obtain the following model:

$$\partial_t \mathbf{u} = D\Delta\mathbf{u} + \alpha(u_1+u_2+v_1+v_2)^\beta G\mathbf{u} + H\mathbf{u} =: D\Delta\mathbf{u} + \mathbf{f}(\mathbf{u}), \tag{4.2}$$

where $x \in \Omega = [0, L] \subset \mathbb{R}$ and $t > 0$, with continuous initial conditions

$$\begin{aligned} u_{10}(x) &= u_1(x,0) \\ u_{20}(x) &= u_2(x,0) \\ v_{10}(x) &= v_1(x,0) \\ v_{20}(x) &= v_2(x,0) \end{aligned} \tag{4.3}$$

and Neumann boundary conditions

$$\begin{aligned} \partial_x u_1(t,0) = \partial_x u_1(t,L) = \partial_x u_2(t,0) = \partial_x u_2(t,L) = 0 \\ \partial_x v_1(t,0) = \partial_x v_1(t,L) = \partial_x v_2(t,0) = \partial_x v_2(t,L) = 0. \end{aligned} \tag{4.4}$$

Remark. Componentwise, the new model (4.2) can be written as follows:

$$\begin{aligned} \partial_t u_1 &= d_{11}\Delta u_1 - \alpha(u_1+u_2+v_1+v_2)^\beta u_1 - au_1 + bu_2 + cv_1 \\ &=: d_{11}\Delta u_1 + f_1(u_1,u_2,v_1,v_2) \\ \partial_t u_2 &= d_{12}\Delta u_2 - \alpha(u_1+u_2+v_1+v_2)^\beta u_2 + au_1 - bu_2 \\ &=: d_{12}\Delta u_2 + f_2(u_1,u_2,v_1,v_2) \\ \partial_t v_1 &= d_{21}\Delta v_1 + r_1\alpha(u_1+u_2+v_1+v_2)^\beta u_1 + r_2\alpha(u_1+u_2+v_1+v_2)^\beta u_2 \\ &\qquad - av_1 + bv_2 - cv_1 \\ &=: d_{21}\Delta v_1 + f_3(u_1,u_2,v_1,v_2) \\ \partial_t v_2 &= d_{22}\Delta v_2 + (1-r_1)\alpha(u_1+u_2+v_1+v_2)^\beta u_1 \\ &\qquad + (1-r_2)\alpha(u_1+u_2+v_1+v_2)^\beta u_2 + av_1 - bv_2, \\ &=: d_{22}\Delta v_2 + f_4(u_1,u_2,v_1,v_2). \end{aligned} \tag{4.5}$$

4.2 Third theorem

Consider the new compartmental model (4.2), with initial conditions (4.3) and Neumann boundary conditions (4.4).

Assume that the power

$$\beta > 1, \tag{4.6}$$

the sinking rates

$$0 \leq r_1, r_2 \leq 1, \tag{4.7}$$

and all other coefficients are positive, i.e.

$$a, b, c, \alpha, d_{11}, d_{12}, d_{21}, d_{22}, L > 0. \tag{4.8}$$

Lemma 4.2.1. *The averaged total mass*

$$s := \frac{1}{|\Omega|} \int_\Omega [u_1(x,t) + u_2(x,t) + v_1(x,t) + v_2(x,t)]\, dx \tag{4.9}$$

is conserved for any $t \geq 0$.

Proof. If we sum up all four equations, we have time-derivatives on the left hand side and the sum of diffusion and reaction terms on the right hand side. The reaction terms on the right hand side are designed to add up to 0 and we have Neumann boundary conditions. Thus, the system (4.2) is mass-conserved, i.e.

$$\begin{aligned} \frac{d}{dt} \int_\Omega (u_1(x,t) + u_2(x,t) + v_1(x,t) + v_2(x,t))\, dx \\ = \int_\Omega (d_{11}\Delta u_1 + d_{12}\Delta u_2 + d_{21}\Delta v_1 + d_{22}\Delta v_2)\, dx = 0, \end{aligned} \tag{4.10}$$

the last identity holds by the integration by parts and Neumann boundary conditions. Hence

$$s := \frac{1}{|\Omega|} \int_\Omega (u_{10}(x) + u_{20}(x) + v_{10}(x) + v_{20}(x))\, dx \tag{4.11}$$

is conserved for any $t \geq 0$. □

The next theorem elucidate how Turing instability is lost, and the associated pattern formation fails under rapidly periodic illumination.

Theorem 4.2.2. *Consider the new compartmental model (4.2), with initial conditions (4.3) and Neumann boundary conditions (4.4), the power condition (4.6), the sinking rate condition (4.7), and the positivity condition (4.8). Then, there exists a unique positive homogeneous equilibrium*

$$\begin{pmatrix} \overline{u_1} \\ \overline{u_2} \\ \overline{v_1} \\ \overline{v_2} \end{pmatrix} \tag{4.12}$$

parametrized by any $s > 0$. The explicit form of the homogeneous equilibrium (4.12) can be found in Appendix A. Assume

$$\det\left(\mathbf{J}_4(\overline{u_1}, \overline{u_2}, \overline{v_1}, \overline{v_2}) - k^2 D\right) < 0 \tag{4.13}$$

for some wave number $k \in \mathbb{N}$. Here, $\mathbf{J}_4$ denotes the Jacobi matrix of the kinetics $\mathbf{f} := (f_1, f_2, f_3, f_4)^\intercal$ of the system (4.2). Then the system has Turing instability.

Moreover, there exists a set of coefficients for which the homogeneous equilibrium (4.12) is stable in the kinetic system of the system (4.2) and $\det(\mathbf{J}(\overline{u_1}, \overline{u_2}, \overline{v_1}, \overline{v_2}) - k^2 D)$ *surpasses* 0 *as the value of* a *approaches the value of* b*, i.e. Turing instability is lost as* a *approaches* b*.*

Proof. Similarly to Proof of Theorem 2.2.2, in (Step 1) we compute the homogeneous equilibrium using the conserved quantity (4.9). In (Step 2), we study the linear stability of the homogeneous equilibrium under homogeneous perturbations. In (Step 3), we study the stability of the homogeneous equilibrium under nonhomogeneous perturbations. In (Step 4), we will present a set of coefficients for which the homogeneous equilibrium (4.12) loses its stability the determinant surpasses 0 as the value of a approaches the value of b.

(Step 1) Consider the homogeneous equilibrium $(\bar{u_1}, \bar{u_2}, \bar{v_1}, \bar{v_2})^\intercal$ of the system (4.2). Note that the sum $f_1 + f_2 + f_3 + f_4$ is identically zero. Hence, it suffices to solve $f_1 + f_2 + f_3 = 0$ at the homogeneous equilibrium $(\bar{u_1}, \bar{u_2}, \bar{v_1}, \bar{v_2})^\intercal$.

Now, the conserved quantity (4.11) satisfies

$$s = \frac{1}{|\Omega|}\int_\Omega (\bar{u_1} + \bar{u_2} + \bar{v_1} + \bar{v_2})\, dx = \bar{u_1} + \bar{u_2} + \bar{v_1} + \bar{v_2}, \tag{4.14}$$

and equations for the first three components read as follows:

$$\begin{aligned} 0 =& -\alpha s^\beta \bar{u_1} - a\bar{u_1} + b\bar{u_2} + c\bar{v_1} \\ 0 =& -\alpha s^\beta \bar{u_2} + a\bar{u_1} - b\bar{u_2} \\ 0 =& r_1\alpha s^\beta \bar{u_1} + r_2\alpha s^\beta \bar{u_2} - a\bar{v_1} + b\bar{v_2} - c\bar{v_1}. \end{aligned} \tag{4.15}$$

We can solve (4.15) as a linear system:

$$B\begin{pmatrix}\bar{u_1}\\ \bar{u_2}\\ \bar{v_1}\end{pmatrix} := \begin{pmatrix}-a-\alpha s^\beta & b & c\\ a & -b-\alpha s^\beta & 0\\ r_1\alpha s^\beta - b & r_2\alpha s^\beta - b & -a-b-c\end{pmatrix}\begin{pmatrix}\bar{u_1}\\ \bar{u_2}\\ \bar{v_1}\end{pmatrix} = \begin{pmatrix}0\\ 0\\ -bs\end{pmatrix}. \tag{4.16}$$

Since

$$\begin{aligned} \det B =& \, r_1\alpha^2 c s^{2\beta} - a\alpha^2 s^{2\beta} - \alpha^2 b s^{2\beta} - \alpha^2 c s^{2\beta} - abc - a^2\alpha s^\beta - \alpha b^2 s^\beta \\ & - b^2 c - 2a\alpha b s^\beta - a\alpha c s^\beta - 2\alpha b c s^\beta + r_2 a\alpha c s^\beta + r_1\alpha b c s^\beta \\ =& -(1-r_1)\alpha^2 c s^{2\beta} - (1-r_2)a\alpha c s^\beta - (1-r_1)\alpha b c s^\beta \\ & - a\alpha^2 s^{2\beta} - \alpha^2 b s^{2\beta} - abc - a^2\alpha s^\beta - \alpha b^2 s^\beta \\ & - b^2 c - 2a\alpha b s^\beta - \alpha b c s^\beta \\ <& \, 0, \end{aligned}$$

we can invert the matrix B to solve for the homogeneous equilibrium (4.12).

The explicit expression can be found in Appendix A.

(Step 2) If we consider the stability of the homogeneous equilibrium (A.5) in the kinetic system of the system (4.2), we obtain a trivial eigenvalue 0 associated with

the eigenvector

$$\begin{pmatrix} 1 \\ 1 \\ 1 \\ 1 \end{pmatrix}. \tag{4.17}$$

We can indeed eliminate the eigenvalue 0, if we reduce the number of components by the mass constraint (4.14), and consider the linear stability of the homogeneous equilibrium (A.5) of the first three components of the kinetic system of the system (4.2):

$$\begin{aligned} \partial_t u_1 &= -\alpha(u_1+u_2+v_1+v_2)^\beta u_1 - a u_1 + b u_2 + c v_1 \\ &= f_1(u_1,u_2,v_1,v_2) \\ \partial_t u_2 &= -\alpha(u_1+u_2+v_1+v_2)^\beta u_2 + a u_1 - b u_2 \\ &= f_2(u_1,u_2,v_1,v_2) \\ \partial_t v_1 &= r_1\alpha(u_1+u_2+v_1+v_2)^\beta u_1 + r_2\alpha(u_1+u_2+v_1+v_2)^\beta u_2 \\ &\qquad - a v_1 + b v_2 - c v_1 \\ &= f_3(u_1,u_2,v_1,v_2). \end{aligned} \tag{4.18}$$

We can compute the Jacobi matrix of the system and the explicitly expression can be found in Appendix A.

Notice that $(u_1,u_2,v_1) \to (\bar{u_1},\bar{u_2},\bar{v_1})$ as $t\to\infty$ implies that $v_2 = s-u_1-u_2-v_1 \to s-\bar{u_1}-\bar{u_2}-\bar{v_1} = \bar{v_2}$ as $t\to\infty$. Therefore, if we have an asymptotically stable equilibrium $(\bar{u_1},\bar{u_2},\bar{v_1})$, then $(\bar{u_1},\bar{u_2},\bar{v_1},\bar{v_2})$ is also asymptotically stable under the constraint of mass (4.14).

We will check the stability of the homogeneous equilibrium (A.5), later with the set of coefficients that gives us an unstable equilibrium under nonhomogeneous perturbations.

(Step 3) Now consider the full reaction-diffusion system and linearize it about the homogeneous equilibrium (A.5). Equivalently, setting

$$w(x,t) = (u_1(x,t),u_2(x,t),v_1(x,t),v_2(x,t))^\intercal - (\bar{u_1},\bar{u_2},\bar{v_1},\bar{v_2})^\intercal, \tag{4.19}$$

$D := \mathrm{diag}(d_{11},d_{12},d_{21},d_{22})$, and $f := (f_1,f_2,f_3,f_4)^\intercal$, we linearize the system

$$\partial_t w = D\Delta w + f(w) \tag{4.20}$$

about the origin $w = (0,0,0,0)^\intercal$. We obtain

$$\partial_t w = D\Delta w + \mathbf{J}_4(\bar{u_1},\bar{u_2},\bar{v_1},\bar{v_2})w, \tag{4.21}$$

where $\mathbf{J}_4$ denotes the Jacobi matrix of $f := (f_1,f_2,f_3,f_4)^\intercal$.

Substituting

$$w = \tilde{w}\exp(\lambda t + ikx), \tag{4.22}$$

into the system (4.21), we study the linear stability of the wave number k:

$$\lambda\tilde{w} = \begin{pmatrix} -k^2 d_{11} + f_{1u_1} & f_{1u_2} & f_{1v_1} & f_{1v_2} \\ f_{2u_1} & -k^2 d_{12} + f_{2u_2} & f_{2v_1} & f_{2v_2} \\ f_{3u_1} & f_{3u_2} & -k^2 d_{21} + f_{3v_1} & f_{3v_2} \\ f_{4u_1} & f_{4u_2} & f_{4v_1} & -k^2 d_{22} + f_{4v_2} \end{pmatrix} \tilde{w} \tag{4.23}$$

$$=: A_k \tilde{w}, \tag{4.24}$$

where derivatives are evaluated at the homogeneous equilibrium. Consider the characteristic polynomial of A_k:

$$\begin{aligned} \Phi(\lambda) &= \det(\lambda I - A_k) \\ &= \lambda^4 + (-\mathrm{tr} A_k)\lambda^3 + p\lambda^2 + q\lambda + (-1)^4 \det(A_k), \end{aligned} \tag{4.25}$$

where p and q are some polynomials in k^2 and coefficients.

If

$$\mathrm{tr} A_k = -k^2(d_{11} + d_{12} + d_{21} + d_{22}) + \mathrm{tr}\mathbf{J}(\bar{u_1}, \bar{u_2}, \bar{v_1}, \bar{v_2}) < 0, \tag{4.26}$$

the value of the characteristic polynomial at $\lambda = 0$:

$$\Phi(0) = \det A_k < 0 \tag{4.27}$$

implies that there exists an eigenvalue with positive real part, depending on the wave number k.

(Step 4) For example, the following set of coefficients realizes the scenario: $s = 3$, $b = 1$, $c = 1$, $\alpha = 1$, $\beta = 2$, $r_1 = 0.9$, $r_2 = 0.8$, $d_{11} = 1$, $d_{12} = 2$, $d_{21} = 0.01$, and $d_{22} = 0.1$. The ratio a/b then determines the sign of $\det A_k$. In particular, the wave number k becomes unstable as the value of a approaches b. Figure 4.2 illustrates how the first mode becomes stable as a approaches b.

Fix $a = 0.2$. Figure 4.2 illustrates which modes grow. For this particular set of coefficients, the wave number k such that $0 \leq k^2 \leq 16$, i.e. $k = 1, 2, 3, 4$ grow exponentially.

Let us check the linear stability of the homogeneous equilibrium under homogeneous perturbations for the set of coefficients $s = 3$, $a = 0.2$, $b = 1$, $c = 1$, $\alpha = 1$, $\beta = 2$, $r_1 = 0.9$, $r_2 = 0.8$, $d_{11} = 1$, $d_{12} = 2$, $d_{21} = 0.01$, and $d_{22} = 0.1$. We can compute the Jacobi matrix

$$\mathbf{J}_3(\bar{u_1}, \bar{u_2}, \bar{v_1}, \bar{v_2}) \tag{4.28}$$

$$= \begin{pmatrix} -2238309/207910 & 2791/20791 & 2791/20791 \\ 170919/207910 & -209530/20791 & -1620/20791 \\ 1859031/207910 & 835956/103955 & -220069/207910 \end{pmatrix}, \tag{4.29}$$

and

$$\det \mathbf{J}_3 = -225748161/2079100 \approx -108.5798, \tag{4.30}$$

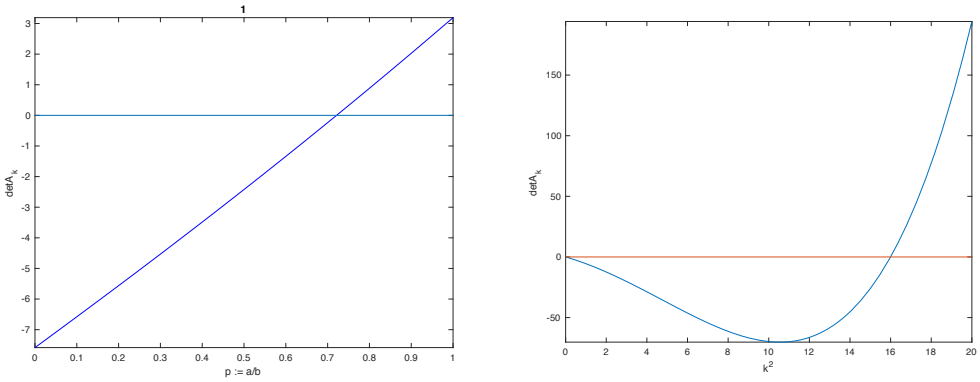

Figure 4.2: $\det A_1$ depending on the ratio of the values a and b. As $p := a/b$ increase from 0 to 1, the value $\det A_1$ surpasses 0. (Left picture); $\det A_k$ depending on the wave number k. The picture shows the wave numbers for which $\det A_k$ is negative, so that eigenvalues with positive real part emerge. (Right picture).

hence the product of the three eigenvalues is away from 0. The numerically calculated eigenvalues are the following:

$$\begin{aligned} \lambda_1 &= -0.9956 - 0.0000i \\ \lambda_2 &= -10.9121 - 0.0000i \\ \lambda_3 &= -9.9944 + 0.0000i, \end{aligned} \tag{4.31}$$

all the eigenvalues are real and strictly negative.

□

4.3 Saturation of linear instability

As well as the Suematsu model without the nonlocal term (2.4), our compartmental model (4.2) also possesses a positively invariant set.

Proposition 4.3.1. *The kinetic system of the system (4.2) possesses a positively invariant set.*

Proof. We consider nullclines under the constraint of conservation of mass $s = u_1 + u_2 + v_1 + v_2$.

We have a positively invariant set K defined by $u_1 \geq 0$, $u_2 \geq 0$, $v_1 \geq 0$, $v_2 \geq 0$, and $u_1 + u_2 + v_1 + v_2 \leq s$.

Observe that along u_1-axis, the arrows face inward. Indeed, the origin $(0, 0, 0, 0)$ lies on the intersection of u_1-nullclines, u_2-nullclines, v_1-nullclines, and v_2-nullclines. In addition, these nullclines do not intersect with any of the four axes except at the origin so that the part of each axis as an edge of the region K is entirely contained in one basic region.

The vector at $(1, 0, 0, 0)$ is $(-\alpha - a, a, \gamma\alpha, (1 - \gamma)\alpha)$ and at all other points the vectors are oriented inward. Notice that except for u_1, the values are non-negative.

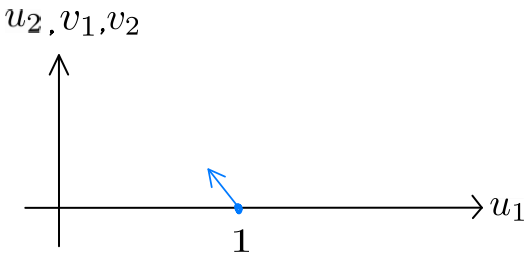

Figure 4.3: Vector field along u_1-axis to illustrate a higher dimensional picture of an inward flux on the axis.

Similarly, along u_2-axis, v_1-axis, and v_2-axis, respectively, the arrows face inward. At $(0,1,0,0)$, the vector is $(b, -\alpha - b, \delta\alpha, (1-\delta)\alpha)$. At $(0,0,1,0)$, the vector is $(c, 0, -a-c, a)$. At $(0,0,0,1)$, the vector is $(0,0,b,-b)$. Notice that except for the value on the axis, other values are non-negative.

Furthermore, the hypersurface defined by the constraint of conservation of mass $u_1 + u_2 + v_1 + v_2 \leq s$ is the upper face. As the homogeneous equilibrium for the kinetics under the mass constraint is stable, it follows that the vector field inside the region never faces out of the region. □

For the full system (4.2), we consider a family of cuboids under the hypersurface $u_1 + u_2 + v_1 + v_2 \leq s$.

Consider an extended system of the system (4.2):

$$\begin{aligned}
\partial_t u_1 &= d_{11}\Delta u_1 - \alpha(u_1+u_2+v_1+v_2)^\beta u_1 - a u_1 + b u_2 + c v_1 \\
&=: d_{11}\Delta u_1 + f_1(u_1,u_2,v_1,v_2) \\
\partial_t u_2 &= d_{12}\Delta u_2 - \alpha(u_1+u_2+v_1+v_2)^\beta u_2 + a u_1 - b u_2 \\
&=: d_{12}\Delta u_2 + f_2(u_1,u_2,v_1,v_2) \\
\partial_t v_1 &= d_{21}\Delta v_1 + r_1\alpha(u_1+u_2+v_1+v_2)^\beta u_1 + r_2\alpha(u_1+u_2+v_1+v_2)^\beta u_2 \\
&\qquad - a v_1 + b v_2 - c v_1 \\
&=: d_{21}\Delta v_1 + f_3(u_1,u_2,v_1,v_2) \\
\partial_t v_2 &= d_{22}\Delta v_2 + (1-r_1)\alpha(u_1+u_2+v_1+v_2)^\beta u_1 \\
&\qquad + (1-r_2)\alpha(u_1+u_2+v_1+v_2)^\beta u_2 + a v_1 - b v_2, \\
&=: d_{22}\Delta v_2 + f_4(u_1,u_2,v_1,v_2) \\
\dot{t} &= 1,
\end{aligned} \tag{4.32}$$

and denote the nonlinearity of this extended system by

$$F(u_1, u_2, v_1, v_2) = \begin{pmatrix} f_1(u_1, u_2, v_1, v_2) \\ f_2(u_1, u_2, v_1, v_2) \\ f_3(u_1, u_2, v_1, v_2) \\ f_4(u_1, u_2, v_1, v_2) \\ 1 \end{pmatrix}. \tag{4.33}$$

Define

$$M := \{(u_1, u_2, v_1, v_2, t) \,|\, (u_1, u_2, v_1, v_2) \in \Gamma(t), t \geq 0\}. \tag{4.34}$$

We will show that the flux at the boundary is inward and apply Lemma 2.3.3.

Remark. We have to deal with a 5-dimensional set, but the argument is similar to that for the 3-dimensional invariant set in the proof of Proposition 2.3.2. To aid visualization, we slightly abuse notation used in Proposition 2.3.2 with an increased number of components for a higher dimensional argument.

Proposition 4.3.2. *Let* $\mathbf{u}_* = (u_{1*}, u_{2*}, v_{1*}, v_{2*})^\intercal \in \partial\Gamma(t)$. *Assume that*

$$\frac{b}{\alpha\beta} \leq {u_{1*}}^{\beta}, \tag{4.35}$$

$$\frac{c}{\alpha\beta} \leq {u_{1*}}^{\beta}, \tag{4.36}$$

and

$$\frac{a}{\alpha\beta} \leq {u_{2*}}^{\beta}. \tag{4.37}$$

Then, the set M *is positively invariant for the extended system.*

Proof. Let h_1 be the first component of the flux vector on the sidewall of the hyper-edge determined by fixing u_{1*} of the 4-dim cross-section Γ_∞. Similarly, let h_2 be the second component, h_3 be the third component, and h_4 be the fourth component, respectively, of the flux vector on the sidewall of the hyper-edge determined by fixing u_{2*}, v_{1*}, v_{2*}, respectively, of the 4-dim cross-section Γ_∞.

Now,

$$h_1 = \langle \eta, \partial_t (u_1, u_2, v_1, v_2, t)^\intercal \rangle = d_{11}\Delta u_1 + f_1(\mathbf{u}_*), \tag{4.38}$$

as $\eta = (1, 0, 0, 0, f_1(\mathbf{u}_*))^\intercal$ on the sidewall of the hyper-edge determined by fixing u_{1*}. Similarly,

$$h_2 = \langle \eta, \partial_t (u_1, u_2, v_1, v_2, t)^\intercal \rangle = d_{12}\Delta u_2 + f_2(\mathbf{u}_*), \tag{4.39}$$

$$h_3 = \langle \eta, \partial_t (u_1, u_2, v_1, v_2, t)^\intercal \rangle = d_{21}\Delta v_1 + f_3(\mathbf{u}_*), \tag{4.40}$$

and

$$h_4 = \langle \eta, \partial_t (u_1, u_2, v_1, v_2, t)^\intercal \rangle = d_{22}\Delta v_2 + f_4(\mathbf{u}_*). \tag{4.41}$$

If we fix u_1, then f_1 has monotonicity in u_2, v_1, and v_2. That is,

$$\partial_{u_2} f_1 = b - \alpha\beta u_1 (u_1 + u_2 + v_1 + v_2)^{\beta - 1} \leq b - \alpha\beta {u_1}_*^{\beta} \leq 0, \tag{4.42}$$

by the assumption (4.35). We have

$$\partial_{v_1} f_1 = c - \alpha\beta u_1(u_1+u_2+v_1+v_2)^{\beta-1} \le c - \alpha\beta u_{1*}^{\beta} \le 0, \tag{4.43}$$

by the assumption (4.36). We also have

$$\partial_{v_2} f_1 = -\alpha\beta u_1(u_1+u_2+v_1+v_2)^{\beta-1} \le 0. \tag{4.44}$$

Therefore, fixing $u_{1*} \in \partial M$, f_1 attains its maximum at $(u_{1*}, 0, 0, 0)$, and

$$f_1(u_{1*}, 0, 0, 0) = -au_{1*} - \alpha u_{1*}^{\beta+1} \le 0. \tag{4.45}$$

Similarly,

$$\partial_{u_1} f_2 = a - \alpha\beta u_2(u_1+u_2+v_1+v_2)^{\beta-1} \le a - \alpha\beta u_{2*}^{\beta} \le 0, \tag{4.46}$$

by the assumption (4.37). We have

$$\partial_{v_1} f_2 = -\alpha\beta u_2(u_1+u_2+v_1+v_2)^{\beta-1} \le 0, \tag{4.47}$$

and

$$\partial_{v_2} f_2 = -\alpha\beta u_2(u_1+u_2+v_1+v_2)^{\beta-1} \le 0. \tag{4.48}$$

Therefore, fixing $u_{2*} \in \partial M$, f_2 attains its maximum at $(0, u_{2*}, 0, 0)$, and

$$f_2(0, u_{2*}, 0, 0) = -bu_{2*} - \alpha u_{2*}^{\beta+1} \le 0. \tag{4.49}$$

Likewise,

$$\begin{aligned}\partial_{u_1} f_3 &= \alpha\beta r_1 u_1(u_1+u_2+v_1+v_2)^{\beta-1} + \alpha r_1(u_1+u_2+v_1+v_2)^{\beta} \\ &\quad + \alpha\beta r_2 u_2(u_1+u_2+v_1+v_2)^{\beta-1} \\ &\ge 0,\end{aligned} \tag{4.50}$$

$$\begin{aligned}\partial_{u_2} f_3 &= \alpha\beta r_1 u_1(u_1+u_2+v_1+v_2)^{\beta-1} + \alpha\beta r_2 u_2(u_1+u_2+v_1+v_2)^{\beta-1} \\ &\quad + \alpha r_2(u_1+u_2+v_1+v_2)^{\beta} \\ &\ge 0,\end{aligned} \tag{4.51}$$

and

$$\begin{aligned}\partial_{v_2} f_3 &= -a + \alpha\beta r_1 u_1(u_1+u_2+v_1+v_2)^{\beta-1} + \alpha\beta r_2 u_2(u_1+u_2+v_1+v_2)^{\beta-1} - c \\ &\ge 0,\end{aligned} \tag{4.52}$$

by assumptions (4.36) and (4.37). Therefore, fixing v_{1*}, f_3 attains its maximum at $(u_{1*}, u_{2*}, v_{1*}, v_{2*})$, and

$$f_3(u_{1*}, u_{2*}, v_{1*}, v_{2*}) = 0 \le 0. \tag{4.53}$$

Again similarly,

$$\begin{aligned}\partial_{u_1} f_4 = &-\alpha\beta r_1 u_1 (u_1+u_2+v_1+v_2)^{\beta-1} - \alpha r_1 (u_1+u_2+v_1+v_2)^{\beta} \\ &- \alpha\beta r_2 u_2 (u_1+u_2+v_1+v_2)^{\beta-1} + \alpha\beta u_1 (u_1+u_2+v_1+v_2)^{\beta-1} \\ &+ \alpha\beta u_2 (u_1+u_2+v_1+v_2)^{\beta-1} + \alpha (u_1+u_2+v_1+v_2)^{\beta} \\ &\geq 0,\end{aligned} \tag{4.54}$$

$$\begin{aligned}\partial_{u_2} f_4 = &-\alpha\beta r_1 u_1 (u_1+u_2+v_1+v_2)^{\beta-1} - \alpha\beta r_2 u_2 (u_1+u_2+v_1+v_2)^{\beta-1} \\ &- \alpha r_2 (u_1+u_2+v_1+v_2)^{\beta} + \alpha\beta u_1 (u_1+u_2+v_1+v_2)^{\beta-1} \\ &+ \alpha\beta u_2 (u_1+u_2+v_1+v_2)^{\beta-1} + \alpha (u_1+u_2+v_1+v_2)^{\beta} \\ &\geq 0,\end{aligned} \tag{4.55}$$

and

$$\begin{aligned}\partial_{v_1} f_4 = &\, a - \alpha\beta r_1 u_1 (u_1+u_2+v_1+v_2)^{\beta-1} - \alpha\beta r_2 u_2 (u_1+u_2+v_1+v_2)^{\beta-1} \\ &+ \alpha\beta u_1 (u_1+u_2+v_1+v_2)^{\beta-1} + \alpha\beta u_2 (u_1+u_2+v_1+v_2)^{\beta-1} \\ &\geq 0.\end{aligned} \tag{4.56}$$

Therefore, fixing v_{2*}, f_4 attains its maximum at $(u_{1*}, u_{2*}, v_{1*}, v_{2*})$, and

$$f_4(u_{1*}, u_{2*}, v_{1*}, v_{2*}) = 0 \leq 0. \tag{4.57}$$

By the maximum principle, we have that Δu_1, Δu_2, Δv_1, and Δv_2 take the maximum value 0 at the boundary. Hence, we have all

$$h_1, h_2, h_3, h_4 \leq 0, \tag{4.58}$$

for $(x,t) \in \Omega \times (0,T]$.

□

Chapter 5

Discussions

In this chapter, we will interpret the result and admit some limitations of our model.

Note that experimental observations are consistent with our hypotheses, which however does not prove the hypotheses. In the sense of Karl Popper, our hypotheses merely stand the test of available experimental data, and have not been falsified.

Finally, we will conclude this thesis with some future directions.

5.1 Interpretation

The Suematsu model without localization for the stationary setting has Turing instability by Theorem 2.2.2 and the effect of rapidly periodic forcing is limited by Theorem 3.3.1.

By Theorem 4.2.2, there is a set of coefficients that realizes the scenario. Namely, considering the density associated to each point of the schematically divided two layers of the cross-section of the sealed container, the bioconvection patterns can be regarded as the exchange of density between the two layers. Moreover, depending on the external illumination conditions, dynamics of the density associated to one of the two directions at each point can also be emulated. Especially, the exchange of density facing either direction within a layer plays a role to form or not form macroscopic patterns.

Varying coupling strength of diffusion, sinking, and vertical swimming, in particular, choosing values of diffusion coefficients, we found a parameter region which seems to be correspondent to the phenomenon we wanted to emulate.

We showed one such set of parameters, namely $s = 3$, $b = 1$, $c = 1$, $\alpha = 1$, $\beta = 2$, $r_1 = 0.9$, $r_2 = 0.8$, $d_{11} = 1$, $d_{12} = 2$, $d_{21} = 0.01$, and $d_{22} = 0.1$. For these coefficients, instability is induced depending on the value of a. If the value of a is small enough, compared with the value of b, the system is Turing unstable; whereas the value of a is large enough, the system is stable. The above is precisely the scenario we expected in the beginning.

Let us start from the following hypothesis. Each cell navigates by light information its sensor receives. If it senses flicker, then it makes a change of direction. If it does not sense flicker, then it keeps swimming. Under stationary illumination, each cell

is able to respond to the environment in such a way its navigation system works well. As a result, vertical swimming is maintained for long enough time, and the top-heavy condition induces convection. Under rapidly periodic illumination, each cell gets confused by our artificial nasty manipulation of the external environment, and vertical swimming weakens, so that the necessary top-heavy condition is no longer satisfied and no convection emerges.

Our unnatural environment causes the confusion of cells and we have found that the rotation of a cell can realize a simple way for the intensity-and-periodicity-based navigation system.

Our system was built based on a hypothesis about the inner mechanism of each cell, namely Euglena gracilis makes a change of direction if and only if it senses flicker. Instead of taking a microscopic viewpoint of biology, we took a macroscopic approach dealing with their collective behavior.

On the other hand, our mathematical analysis is an evidence of the hypothesis based on our thought experiment,

and we hope that our hypothesis will be supported by future experiments.

We hope that a quantitative analysis supported by the wet lab experiments confirm our theoretical result.

5.1.1 Suematsu model

Retrospectively, we notice that the Suematsu model without the nonlocal term (2.4) is a special case of our new model: All cells are vertical and there is no dynamics of directions. In other words, First theorem is a corollary of Third theorem.

Relative positions of cells and their dynamics turned out to be crucial to explain patterns in the periodic setting, which then provides us with an insight into the inner mechanism of phototaxis, even under stationary setting, where the Suematsu model is able to describe the phenomenon very well.

The stationary illumination from below is already unnatural, in the sense the navigation system of Euglena gracilis must have developed for the natural environment in the daylight. Usually, the sunshine illuminates the earth from above and it is beneficial for plants to synthesize energy. Nevertheless, in that environment, an interesting bioconvection pattern was observed in the laboratory, which attracted people studying the mechanism of the collective behavior. Rapidly periodic illumination from below is even more unnatural. However, studying this rather artificial setting, we are able to test the mechanism of negative phototaxis.

5.1.2 Stigmaless mutants

We assumed a definitive role of the stigma. If the periodic shading of the sensor by the stigma is absent, our hypothesis has to be modified.

However, even if stigmaless mutants can also orient with respect to the light direction, and negative phototaxis does not need a stigma, our assumptions are not necessary contradictory.

Indeed, we assumed that a cell keeps swimming if it does not sense flicker. In other words, a cell does not need its stigma unless it wants to make a change of direction.

Without the ability of making a change of direction, we expect different macroscopic patterns, and further experiments are desired.

5.2 Limitations

In this thesis, there are many features we had to discard.

First, we only considered two relative positions of a cell. Recall Figure 1.7. However, the absorption of light the chloroplast might have an influence on the information the sensor receives, and this information might help a cell to determine if it faces toward or away from the light source. It is worth investigating the two cases, assuming some rules of responses depending on whether a cell faces toward or away from the light source.

Second, we assumed that all cells of Euglena gracilis swim at a constant speed. However, it is known that the speed of swimming depends on the environment, and such response is called photokinesis. Euglena gracilis is also known to show fatigue, which is not so surprising to human beings, and also cells can get older. Moreover, randomness of their movement was only implicitly included in our model as diffusion.

Third, even though the de facto standard of the governing equations for fluid is the Navier–Stokes equations, we adopted an approach using a reaction-diffusion system. Eventually, though, it would be great if one could unify bioconvection from fluid dynamics' point of view and bioconvection from reaction-diffusion systems' point of view.

5.3 Future directions

As future directions, the following are worth investigation:

(i) Study permissible perturbations to our new system by a drift term,

(ii) Push ahead with the modeling part furthermore, and

(iii) Include stochasticity into our model.

5.3.1 Perturbations

Although we discarded the nonlocal term of the Suematsu model in my dissertation, one can argue that nonlocal interactions such as the self-shading effect should play a role to form patterns.

Perturbation of the steady state of the Suematsu system (2.4) by the nonlocal term was studied in [Tok17], and it turned out that the effect of the nonlocal term on the equilibrium of the system under stationary illumination was limited.

However, it might have some influence on the transient or equilibrium of our extended system. Moreover, localization itself is interesting and worth further studies.

5.3.2 Modeling

As the next step, we should consider configurations continuously dependent on the angle of the vertical line and the long axis of the cell. This would make the model more complicated as it involves a transport equation to describe the angular interactions. Transport equations in biology have been attracting much attention [Per07], and I would like to make a progress in this direction.

I would also like to regard non-pattern formation under periodic illumination as a resonance phenomenon. Resonance phenomena appear also in biology. For example, the frequency at which a dog pants is close to the resonant frequency of its respiratory system, which causes the maximum amount of air to move in and out of the dog and minimizes the effort that the dog must exert to cool itself [YF12]. By analogy, the frequency at which Euglena gracilis self-rotates might be close to the resonant frequency of its internal signaling system, which could make it possible for such a primitive microorganism to distinguish rapid oscillatory illumination from stationary illumination.

5.3.3 Stochasticity

Stochasticity can be included in addition to diffusion to model randomness of movement. The stochastic nature of the movement of Euglena gracilis was reported by [RRS$^+$15]. Euglena gracilis swims by swinging its flagellum around and generates active fluctuations due to internal random performance of the propulsive motor, resulting in the stochastic nature of the movement.

Models of the chemotaxis view the chemotactic response as analogous to Brownian motion [KS71]. However, one must be careful as the cell of Euglena gracilis is much bigger than water molecules and thus Brownian motion should be negligible, at least to the cell itself as a particle. Also, notice the fundamental differences of chemotaxis and phototaxis. For instance, chemical substances stay at a particular moment to generate the gradient of concentration but light travels much faster than chemical substances. Statistical physical arguments may be necessary to describe how the sensor receives light.

Appendix A

Explicit expressions

Here, explicit expressions of the homogeneous equilibrium (A.5) and of the Jacobi matrix at the homogeneous equilibrium (A.8) in the proof of Theorem 4.2.2 can be found.

A.1 Homogeneous equilibrium

Since

$$\det B < 0,$$

we can invert the matrix B to solve for the homogeneous equilibrium (4.12) as follows:

$$\begin{pmatrix} \bar{u_1} \\ \bar{u_2} \\ \bar{v_1} \end{pmatrix} = B^{-1} \begin{pmatrix} 0 \\ 0 \\ -bs \end{pmatrix} = \frac{1}{\det B} \mathrm{Adj} B \begin{pmatrix} 0 \\ 0 \\ -bs \end{pmatrix}, \tag{A.1}$$

where the adjugate denotes the transpose of its cofactor matrix.

Here the cofactor matrix of the 3×3 matrix

$$\begin{pmatrix} a_{11} & a_{12} & a_{13} \\ a_{21} & a_{22} & a_{23} \\ a_{31} & a_{32} & a_{33} \end{pmatrix} \tag{A.2}$$

is

$$\mathbf{C} = \begin{pmatrix} +\det \begin{pmatrix} a_{22} & a_{23} \\ a_{32} & a_{33} \end{pmatrix} & -\det \begin{pmatrix} a_{21} & a_{23} \\ a_{31} & a_{33} \end{pmatrix} & +\det \begin{pmatrix} a_{21} & a_{22} \\ a_{31} & a_{32} \end{pmatrix} \\ -\det \begin{pmatrix} a_{12} & a_{13} \\ a_{32} & a_{33} \end{pmatrix} & +\det \begin{pmatrix} a_{11} & a_{13} \\ a_{31} & a_{33} \end{pmatrix} & -\det \begin{pmatrix} a_{11} & a_{12} \\ a_{31} & a_{32} \end{pmatrix} \\ +\det \begin{pmatrix} a_{12} & a_{13} \\ a_{22} & a_{23} \end{pmatrix} & -\det \begin{pmatrix} a_{11} & a_{13} \\ a_{21} & a_{23} \end{pmatrix} & +\det \begin{pmatrix} a_{11} & a_{12} \\ a_{21} & a_{22} \end{pmatrix} \end{pmatrix}, \tag{A.3}$$

and the adjugate is

$$\begin{aligned}
&\operatorname{Adj}\begin{pmatrix} a_{11} & a_{12} & a_{13} \\ a_{21} & a_{22} & a_{23} \\ a_{31} & a_{32} & a_{33} \end{pmatrix} \\
&= \mathbf{C}^{\intercal} = \begin{pmatrix} +\det\begin{pmatrix} a_{22} & a_{23} \\ a_{32} & a_{33} \end{pmatrix} & -\det\begin{pmatrix} a_{12} & a_{13} \\ a_{32} & a_{33} \end{pmatrix} & +\det\begin{pmatrix} a_{12} & a_{13} \\ a_{22} & a_{23} \end{pmatrix} \\ -\det\begin{pmatrix} a_{21} & a_{23} \\ a_{31} & a_{33} \end{pmatrix} & +\det\begin{pmatrix} a_{11} & a_{13} \\ a_{31} & a_{33} \end{pmatrix} & -\det\begin{pmatrix} a_{11} & a_{13} \\ a_{21} & a_{23} \end{pmatrix} \\ +\det\begin{pmatrix} a_{21} & a_{22} \\ a_{31} & a_{32} \end{pmatrix} & -\det\begin{pmatrix} a_{11} & a_{12} \\ a_{31} & a_{32} \end{pmatrix} & +\det\begin{pmatrix} a_{11} & a_{12} \\ a_{21} & a_{22} \end{pmatrix} \end{pmatrix}.
\end{aligned} \tag{A.4}$$

Explicitly, homogeneous equilibrium (A.1) can be written in terms of $s > 0$ as follows:

$$\begin{aligned}
\bar{u_1}(s) &= (bcs(b+\alpha s^{\beta}))/(b^2c + a\alpha^2 s^{2\beta} + \alpha^2 b s^{2\beta} + \alpha^2 c s^{2\beta} + abc + a^2\alpha s^{\beta} \\
&\quad + \alpha b^2 s^{\beta} - \alpha^2 c r_1 s^{2\beta} + 2a\alpha b s^{\beta} + a\alpha c s^{\beta} + 2\alpha bc s^{\beta} - a\alpha c r_2 s^{\beta} - \alpha bc r_1 s^{\beta}) \\
\bar{u_2}(s) &= (abcs)/(b^2c + a\alpha^2 s^{2\beta} + \alpha^2 b s^{2\beta} + \alpha^2 c s^{2\beta} + abc + a^2\alpha s^{\beta} + \alpha b^2 s^{\beta} \\
&\quad - \alpha^2 c r_1 s^{2\beta} + 2a\alpha b s^{\beta} + a\alpha c s^{\beta} + 2\alpha bc s^{\beta} - a\alpha c r_2 s^{\beta} - \alpha bc r_1 s^{\beta}), \\
\bar{v_1}(s) &= (bs(\alpha^2 s^{2\beta} + a\alpha s^{\beta} + \alpha b s^{\beta}))/(b^2c + a\alpha^2 s^{2\beta} + \alpha^2 b s^{2\beta} + \alpha^2 c s^{2\beta} + abc + a^2\alpha s^{\beta} \\
&\quad + \alpha b^2 s^{\beta} - \alpha^2 c r_1 s^{2\beta} + 2a\alpha b s^{\beta} + a\alpha c s^{\beta} + 2\alpha bc s^{\beta} - a\alpha c r_2 s^{\beta} - \alpha bc r_1 s^{\beta}), \\
\bar{v_2}(s) &= s - \bar{u_1}(s) - \bar{u_2}(s) - \bar{v_1}(s) \\
&= s - (bs(\alpha^2 s^{2\beta} + a\alpha s^{\beta} + \alpha b s^{\beta}))/(b^2c + a\alpha^2 s^{2\beta} + \alpha^2 b s^{2\beta} + \alpha^2 c s^{2\beta} + abc \\
&\quad + a^2\alpha s^{\beta} + \alpha b^2 s^{\beta} - \alpha^2 c r_1 s^{2\beta} + 2a\alpha b s^{\beta} + a\alpha c s^{\beta} + 2\alpha bc s^{\beta} - a\alpha c r_2 s^{\beta} - \alpha bc r_1 s^{\beta}) \\
&\quad - (abcs)/(b^2c + a\alpha^2 s^{2\beta} + \alpha^2 b s^{2\beta} + \alpha^2 c s^{2\beta} + abc + a^2\alpha s^{\beta} + \alpha b^2 s^{\beta} - \alpha^2 c r_1 s^{2\beta} \\
&\quad + 2a\alpha b s^{\beta} + a\alpha c s^{\beta} + 2\alpha bc s^{\beta} - a\alpha c r_2 s^{\beta} - \alpha bc r_1 s^{\beta}) \\
&\quad - (bcs(b+\alpha s^{\beta}))/(b^2c + a\alpha^2 s^{2\beta} + \alpha^2 b s^{2\beta} + \alpha^2 c s^{2\beta} + abc + a^2\alpha s^{\beta} + \alpha b^2 s^{\beta} \\
&\quad - \alpha^2 c r_1 s^{2\beta} + 2a\alpha b s^{\beta} + a\alpha c s^{\beta} + 2\alpha bc s^{\beta} - a\alpha c r_2 s^{\beta} - \alpha bc r_1 s^{\beta}).
\end{aligned} \tag{A.5}$$

A.2 Jacobi matrix at the homogeneous equilibrium (A.5)

We can compute the Jacobi matrix of the system as follows:

$$\mathbf{J}_3 = \begin{pmatrix} J_{11} & J_{12} & J_{13} \\ J_{21} & J_{22} & J_{23} \\ J_{31} & J_{32} & J_{33} \end{pmatrix}, \tag{A.6}$$

where

$$
\begin{aligned}
J_{11} &= -a - \alpha(u_1+u_2+v_1+v_2)^{\beta} - \alpha\beta u_1(u_1+u_2+v_1+v_2)^{\beta-1} \\
J_{12} &= b - \alpha\beta u_1(u_1+u_2+v_1+v_2)^{\beta-1} \\
J_{13} &= c - \alpha\beta u_1(u_1+u_2+v_1+v_2)^{\beta-1} \\
J_{21} &= a - \alpha\beta u_2(u_1+u_2+v_1+v_2)^{\beta-1} \\
J_{22} &= -b - \alpha(u_1+u_2+v_1+v_2)^{\beta} - \alpha\beta u_2(u_1+u_2+v_1+v_2)^{\beta-1} \\
J_{23} &= -\alpha\beta u_2(u_1+u_2+v_1+v_2)^{\beta-1} \\
J_{31} &= \alpha r_1(u_1+u_2+v_1+v_2)^{\beta} + \alpha\beta r_1 u_1(u_1+u_2+v_1+v_2)^{\beta-1} \\
&\quad + \alpha\beta r_2 u_2(u_1+u_2+v_1+v_2)^{\beta-1} \\
J_{32} &= \alpha r_2(u_1+u_2+v_1+v_2)^{\beta} + \alpha\beta r_1 u_1(u_1+u_2+v_1+v_2)^{\beta-1} \\
&\quad + \alpha\beta r_2 u_2(u_1+u_2+v_1+v_2)^{\beta-1} \\
J_{33} &= \alpha\beta r_1 u_1(u_1+u_2+v_1+v_2)^{\beta-1} - c - a + \alpha\beta r_2 u_2(u_1+u_2+v_1+v_2)^{\beta-1}
\end{aligned}
\tag{A.7}
$$

and substituting the homogeneous equilibrium (A.5) into the Jacobi matrix, we have

$$
\begin{aligned}
&J_{11}(\bar{u_1}(s),\bar{u_2}(s),\bar{v_1}(s),\bar{v_2}(s))\\
&=-a-\alpha s^{\beta}-(\alpha b\beta css^{\beta-1}(b+\alpha s^{\beta}))/(b^2c+a\alpha^2s^{2\beta}+\alpha^2bs^{2\beta}+\alpha^2cs^{2\beta}+abc\\
&+a^2\alpha s^{\beta}+\alpha b^2s^{\beta}-\alpha^2cr_1s^{2\beta}+2a\alpha bs^{\beta}+a\alpha cs^{\beta}+2\alpha bcs^{\beta}-a\alpha cr_2s^{\beta}-\alpha bcr_1s^{\beta})\\
&J_{12}(\bar{u_1}(s),\bar{u_2}(s),\bar{v_1}(s),\bar{v_2}(s))\\
&=b-(\alpha b\beta css^{\beta-1}(b+\alpha s^{\beta}))/(b^2c+a\alpha^2s^{2\beta}+\alpha^2bs^{2\beta}+\alpha^2cs^{2\beta}+abc+a^2\alpha s^{\beta}+\alpha b^2s^{\beta}\\
&-\alpha^2cr_1s^{2\beta}+2a\alpha bs^{\beta}+a\alpha cs^{\beta}+2\alpha bcs^{\beta}-a\alpha cr_2s^{\beta}-\alpha bcr_1s^{\beta})\\
&J_{13}(\bar{u_1}(s),\bar{u_2}(s),\bar{v_1}(s),\bar{v_2}(s))\\
&=c-(\alpha b\beta css^{\beta-1}(b+\alpha s^{\beta}))/(b^2c+a\alpha^2s^{2\beta}+\alpha^2bs^{2\beta}+\alpha^2cs^{2\beta}+abc+a^2\alpha s^{\beta}+\alpha b^2s^{\beta}\\
&-\alpha^2cr_1s^{2\beta}+2a\alpha bs^{\beta}+a\alpha cs^{\beta}+2\alpha bcs^{\beta}-a\alpha cr_2s^{\beta}-\alpha bcr_1s^{\beta})\\
&J_{21}(\bar{u_1}(s),\bar{u_2}(s),\bar{v_1}(s),\bar{v_2}(s))\\
&=a-(a\alpha b\beta css^{\beta-1})/(b^2c+a\alpha^2s^{2\beta}+\alpha^2bs^{2\beta}+\alpha^2cs^{2\beta}+abc+a^2\alpha s^{\beta}+\alpha b^2s^{\beta}\\
&-\alpha^2cr_1s^{2\beta}+2a\alpha bs^{\beta}+a\alpha cs^{\beta}+2\alpha bcs^{\beta}-a\alpha cr_2s^{\beta}-\alpha bcr_1s^{\beta})\\
&J_{22}(\bar{u_1}(s),\bar{u_2}(s),\bar{v_1}(s),\bar{v_2}(s))\\
&=-b-\alpha s^{\beta}-(a\alpha b\beta css^{\beta-1})/(b^2c+a\alpha^2s^{2\beta}+\alpha^2bs^{2\beta}+\alpha^2cs^{2\beta}+abc+a^2\alpha s^{\beta}\\
&+\alpha b^2s^{\beta}-\alpha^2cr_1s^{2\beta}+2a\alpha bs^{\beta}+a\alpha cs^{\beta}+2\alpha bcs^{\beta}-a\alpha cr_2s^{\beta}-\alpha bcr_1s^{\beta})\\
&J_{23}(\bar{u_1}(s),\bar{u_2}(s),\bar{v_1}(s),\bar{v_2}(s))\\
&=-(a\alpha b\beta css^{\beta-1})/(b^2c+a\alpha^2s^{2\beta}+\alpha^2bs^{2\beta}+\alpha^2cs^{2\beta}+abc+a^2\alpha s^{\beta}+\alpha b^2s^{\beta}\\
&-\alpha^2cr_1s^{2\beta}+2a\alpha bs^{\beta}+a\alpha cs^{\beta}+2\alpha bcs^{\beta}-a\alpha cr_2s^{\beta}-\alpha bcr_1s^{\beta})\\
&J_{31}(\bar{u_1}(s),\bar{u_2}(s),\bar{v_1}(s),\bar{v_2}(s))\\
&=\alpha r_1s^{\beta}+(a\alpha b\beta cr_2ss^{\beta-1})/(b^2c+a\alpha^2s^{2\beta}+\alpha^2bs^{2\beta}+\alpha^2cs^{2\beta}+abc+a^2\alpha s^{\beta}+\alpha b^2s^{\beta}\\
&-\alpha^2cr_1s^{2\beta}+2a\alpha bs^{\beta}+a\alpha cs^{\beta}+2\alpha bcs^{\beta}-a\alpha cr_2s^{\beta}-\alpha bcr_1s^{\beta})\\
&+(\alpha b\beta cr_1ss^{\beta-1}(b+\alpha s^{\beta}))/(b^2c+a\alpha^2s^{2\beta}+\alpha^2bs^{2\beta}+\alpha^2cs^{2\beta}+abc+a^2\alpha s^{\beta}+\alpha b^2s^{\beta}\\
&-\alpha^2cr_1s^{2\beta}+2a\alpha bs^{\beta}+a\alpha cs^{\beta}+2\alpha bcs^{\beta}-a\alpha cr_2s^{\beta}-\alpha bcr_1s^{\beta})\\
&J_{32}(\bar{u_1}(s),\bar{u_2}(s),\bar{v_1}(s),\bar{v_2}(s))\\
&=\alpha r_2s^{\beta}+(a\alpha b\beta cr_2ss^{\beta-1})/(b^2c+a\alpha^2s^{2\beta}+\alpha^2bs^{2\beta}+\alpha^2cs^{2\beta}+abc+a^2\alpha s^{\beta}+\alpha b^2s^{\beta}\\
&-\alpha^2cr_1s^{2\beta}+2a\alpha bs^{\beta}+a\alpha cs^{\beta}+2\alpha bcs^{\beta}-a\alpha cr_2s^{\beta}-\alpha bcr_1s^{\beta})\\
&+(\alpha b\beta cr_1ss^{\beta-1}(b+\alpha s^{\beta}))/(b^2c+a\alpha^2s^{2\beta}+\alpha^2bs^{2\beta}+\alpha^2cs^{2\beta}+abc+a^2\alpha s^{\beta}+\alpha b^2s^{\beta}\\
&-\alpha^2cr_1s^{2\beta}+2a\alpha bs^{\beta}+a\alpha cs^{\beta}+2\alpha bcs^{\beta}-a\alpha cr_2s^{\beta}-\alpha bcr_1s^{\beta})\\
&J_{33}(\bar{u_1}(s),\bar{u_2}(s),\bar{v_1}(s),\bar{v_2}(s))\\
&=(a\alpha b\beta cr_2ss^{\beta-1})/(b^2c+a\alpha^2s^{2\beta}+\alpha^2bs^{2\beta}+\alpha^2cs^{2\beta}+abc+a^2\alpha s^{\beta}+\alpha b^2s^{\beta}\\
&-\alpha^2cr_1s^{2\beta}+2a\alpha bs^{\beta}+a\alpha cs^{\beta}+2\alpha bcs^{\beta}-a\alpha cr_2s^{\beta}-\alpha bcr_1s^{\beta})\\
&-c-a+(\alpha b\beta cr_1ss^{\beta-1}(b+\alpha s^{\beta}))/(b^2c+a\alpha^2s^{2\beta}+\alpha^2bs^{2\beta}+\alpha^2cs^{2\beta}+abc+a^2\alpha s^{\beta}\\
&+\alpha b^2s^{\beta}-\alpha^2cr_1s^{2\beta}+2a\alpha bs^{\beta}+a\alpha cs^{\beta}+2\alpha bcs^{\beta}-a\alpha cr_2s^{\beta}-\alpha bcr_1s^{\beta}).
\end{aligned}
\tag{A.8}
$$

Bibliography

[BvdDW08] Fred Brauer, Pauline van den Driessche, and J. Wu, editors. *Mathematical Epidemiology*. Springer-Verlag Berlin Heidelberg, 2008.

[CDBDK90] V. Castets, E. Dulos, J. Boissonade, and P. De Kepper. Experimental evidence of a sustained standing turing-type nonequilibrium chemical pattern. *Phys. Rev. Lett.*, 64:2953–2956, Jun 1990.

[CH93] M. C. Cross and P. C. Hohenberg. Pattern formation outside of equilibrium. *Rev. Mod. Phys.*, 65:851–1112, Jul 1993.

[FT98] Andrew B. Ferrari and Edriss S. Titi. Gevrey regularity for nonlinear analytic parabolic equations. *Communications in Partial Differential Equations*, 23(1 & 2):1–16, 1998.

[GM72] A. Gierer and H. Meinhardt. A theory of biological pattern formation. *Kybernetik*, 12:30–39, 1972.

[Hen81] Daniel Henry. *Geometric Theory of Semilinear Parabollic Equations*. Springer-Verlag Berlin Heidelberg, 1981.

[IOM07] Shuji Ishihara, Mikiya Otsuji, and Atsushi Mochizuki. Transient and steady state of mass-conserved reaction-diffusion systems. *Phys. Rev. E*, 75:015203, Jan 2007.

[KA95] Shigeru Kondo and Rihito Asai. A reaction–diffusion wave on the skin of the marine angelfish pomacanthus. *Nature*, 376(6543):765–768, 1995.

[KCDB91] P. De Kepper, V. Castets, E. Dulos, and J. Boissonade. Turing-type chemical patterns in the chlorite-iodide-malonic acid reaction. *Physica D: Nonlinear Phenomena*, 49(1):161 – 169, 1991.

[KS71] Evelyn F. Keller and Lee A. Segel. Model for chemotaxis. *J. theor. Biol.*, 30:225–234, 1971.

[Mat01] Karsten Matthies. Time-averaging under fast periodic forcing of parabolic partial differential equations: Exponential estimates. *Journal of Differential Equations*, 174(1):133 – 180, 2001.

[Mat08] Karsten Matthies. Exponential averaging under rapid quasiperiodic forcing. *Adv. Differential Equations*, 13(5-6):427–456, 2008.

[MO10] Yoshihisa Morita and Toshiyuki Ogawa. Stability and bifurcation of nonconstant solutions to a reaction-diffusion system with conservation of mass. *Nonlinearity*, 23(6):1387–1411, 2010.

[Mur02] James D. Murray. *Mathematical Biology I: An Introduction*. Springer-Verlag New York, third edition, 2002.

[Mur03] James D. Murray. *Mathematical Biology II: Spatial Models and Biomedical Applications*. Springer-Verlag New York, third edition, 2003.

[Oga10] Toshiyuki Ogawa. *Nonlinear phenomena and differential equations, bifurcation analysis of pattern dynamics (in Japanese, Hisenkeigenshou to Bibunhouteishiki, Patan-dainamikusu no Bunkikaiseki)*. Saiensusha, 2010.

[OIC+07] Mikiya Otsuji, Shuji Ishihara, Carl Co, Kozo Kaibuchi, Atsushi Mochizuki, and Shinya Kuroda. A mass conserved reaction–diffusion system captures properties of cell polarity. *PLoS Computational Biology*, 3:1040–1054, 2007.

[Per07] Benoît Perthame. *Transport Equations in Biology*. Birkhäuser Verlag, 2007.

[Per15] Benoît Perthame. *Parabolic Equations in Biology: Growth, Reaction, Movement and Diffusion*. Springer International Publishing Switzerland, 2015.

[RRS+15] Pawel Romanczuk, Maksym Romenskyy, Dimitri Scholz, Vladimir Lobaskin, and Lutz Schimansky-Geier. Motion of euglena gracilis: Active fluctuations and velocity distribution. *The European Physical Journal Special Topics*, 224, 02 2015.

[SAI+11] Nobuhiko J. Suematsu, Akinori Awazu, Shunsuke Izumi, Shuhei Noda, Satoshi Nakata, and Hiraku Nishimori. Local bioconvection of euglena caused by phototaxis in the lateral direction. *Journal of the Physical Society of Japan*, 2011.

[SS17] Steven D. Schwartzbach and Shigeru Shigeoka, editors. *Euglena: Biochemistry, Cell and Molecular Biology*. Springer International Publishing, 2017.

[Tem88] Roger Temam. *Infinite-Dimensional Dynamical Systems in Mechanics and Physics*. Springer-Verlag New York Inc., 1988.

[Tok17] Yuya M. Tokuta. *Bioconvection Generated by Euglena Gracilis under Stationary Illumination from the Bottom.* Master's thesis, Freie Universität Berlin, 2017.

[Tur52] Alan M. Turing. The chemical basis of morphogenesis. *Philosophical Transactions of the Royal Society of London*, 237(641):37–72, 1952.

[Wei75] Hans F. Weinberger. Invariant sets for weakly coupled parabolic and elliptic systems. *Rendiconti di Matematica*, 8(1):295–310, 1975.

[Yan15] Eiji Yanagida. *Reaction-Diffusion Equations (in Japanese, Hannou Kakusan Houteishiki).* University of Tokyo Press, 2015.

[YF12] Hugh D. Young and Roger A. Freedman. *Sears and Zemansky's University Physics with Modern Physics.* Addison-Wesley, thirteenth edition, 2012.

Deutsche Zusammenfassung

Mittels Modellierung und mathematischer Analyse untersucht diese Doktorarbeit die negative Phototaxis bei Euglena gracilis und die daraus resultierenden Biokonvektionsmuster unter stationärer oder periodischer Illumination.

Diese Dissertation liefert eine neue biologische Hypothese über den Mechanismus der negativen Phototaxis bei Euglena gracilis. Darüberhinaus erklärt sie die ausbleibende Musterbildung bei schneller periodischer Illumination wie sie im Experiment beobachtet wurde.

Ein existierendes Modellgleichungssystem für Muster unter stationärer Illumination wird so erweitert, dass es nun sowohl stationäre als auch schnelle periodische Illumination beschreibt. Das neue Modell weist eine Turing-Instabilität für Koeffizienten auf, die einer stationären Illumination entsprechen, und verliert diese, wenn die Koeffizienten durch solche, die der schnellen periodischen Illumination entsprechen, ersetzt werden. Das Ausbleiben der Musterbildung bei der schnellen periodischen Illumination kann als Verlust der Turing-Instabilität interpretiert werden.

Selbstständigkeitserklärung

Hiermit bestätige ich, TOKUTA, Yuya, dass ich die vorliegende Dissertation mit dem Thema

Negative Phototaxis of Euglena Gracilis and Resulting Bioconvection Patterns under Stationary or Rapidly Periodic Illumination

selbstständig angefertigt und nur die genannten Quellen und Hilfen verwendet habe. Die Arbeit ist erstmalig und nur an der Freien Universität Berlin eingereicht worden.

Berlin, den